

State of Global Water Resources 2022 Report



WEATHER CLIMATE WATER



WORLD
METEOROLOGICAL
ORGANIZATION

WMO-No. 1333

WMO-No. 1333

© World Meteorological Organization, 2023

The right of publication in print, electronic and any other form and in any language is reserved by WMO. Short extracts from WMO publications may be reproduced without authorization, provided that the complete source is clearly indicated. Editorial correspondence and requests to publish, reproduce or translate this publication in part or in whole should be addressed to:

Chair, Publications Board
World Meteorological Organization (WMO)
7 bis, avenue de la Paix
P.O. Box 2300
CH-1211 Geneva 2, Switzerland

Tel.: +41 (0) 22 730 84 03
Email: publications@wmo.int

ISBN 978-92-63-11333-7

Cover illustration from WMO 2024 Calendar Competition: "Climate Change and our Empty Hand" by Malia Zerk (Afghanistan), Faiz Abad, Badakhshan, Afghanistan. This image was modified by generative AI in Adobe Photoshop.

NOTE

The designations employed in WMO publications and the presentation of material in this publication do not imply the expression of any opinion whatsoever on the part of WMO concerning the legal status of any country, territory, city or area, or of its authorities, or concerning the delimitation of its frontiers or boundaries.

The mention of specific companies or products does not imply that they are endorsed or recommended by WMO in preference to others of a similar nature which are not mentioned or advertised.

The findings, interpretations and conclusions expressed in WMO publications with named authors are those of the authors alone and do not necessarily reflect those of WMO or its Members.

Contents

Acknowledgements	ii
List of abbreviations	v
Executive summary	vi
Foreword	viii
Introduction	1
Data sources and anomaly calculation	2
The backdrop: overview of climatic conditions in 2022	3
River discharge	5
Reservoirs	10
Groundwater levels	12
Soil moisture	14
Evapotranspiration	16
Terrestrial water storage	18
Snow cover and glaciers	20
Central Europe and the Alps	20
Subtropical Andes	21
Cryosphere changes and water resources management in Central Asia	22
High-impact hydrological events	26
Pakistan, India and Bangladesh floods	26
Sahel floods	27
Drought in the Horn of Africa and Central Africa	27
Extreme and long-term drought in La Plata basin	27
Summer heatwave in Europe.	27
Synthesis	28
Endnotes	32
Annex 1. Technical annex	37
Annex 2. Quantitative status of groundwater	54

Acknowledgements

WMO is grateful to the following contributors.

WMO MEMBER STATES AND TERRITORIES THROUGH HYDROLOGICAL ADVISORS AND ASSIGNED FOCAL POINTS FOR THE STATE OF GLOBAL WATER RESOURCES REPORT

Armenia; Australia; Belgium; Belize; Benin; Bhutan; Botswana; Brazil; Bulgaria; Canada; China; Colombia; Croatia; Czechia; Denmark; Egypt; France; Germany; Ghana; Hong Kong, China; Hungary; Iceland; India; Kazakhstan; Kenya; Republic of Korea; Latvia; Malawi; Mauritius; Republic of Moldova; Montenegro; Myanmar; Nepal; New Zealand; Norway; Paraguay; Peru; Philippines; Poland; Singapore; Slovenia; South Africa; Sri Lanka; Sweden; Switzerland; Tajikistan; Thailand; United Kingdom of Great Britain and Northern Ireland; United Republic of Tanzania; United States of America; Uruguay; Uzbekistan. Hydrological advisors and focal points contributed to and supported the preparation of the present report by providing observational data, information about major hydrological events that occurred in 2022 and other relevant information, and participated in the review and validation of the report.

STEERING COMMITTEE MEMBERS

Jan Danhelka (Czechia, Chair of the Hydrological Coordination Panel); Harry Dixon (United Kingdom); Michel Jean (Canada, President of INFCOM); Harry Lins (United States); Ian Lisk (United Kingdom, President of SERCOM); Ilias Pechlivanidis (Sweden, Research Board); Silvano Pecora (Italy, Chair of the Joint Expert Team on Hydrological Monitoring); Marcelo Uriburu Quirno (Argentina, Vice-Chair of the Standing Committee on Hydrological Services); Yuri Simonov (Russian Federation, Chair of the Standing Committee on Hydrological Services); Narendra Tuteja (Australia); and Andy Woods (United States, Joint Expert Team on Hydrological Monitoring).

REGIONAL HYDROLOGICAL ADVISORS

Angela Corina (Region VI), John Fenwick (Region V), Sung Kim (Region II), Jean Claude Ntonga (Region I), Fabio Andres Bernal Quiroga (Region III), and Jose Zuniga (Region IV), who contributed to the preparation and review of the report.

WMO EXPERTS

Experts from the Joint Expert Team on Hydrological Monitoring, Study Group on Integrated Energy Services, Standing Committee on Hydrological Services, and Standing Committee on Services for Agriculture, who participated in the preparation and review of the report.



MEMBERS OF THE GLOBAL HYDROLOGICAL MODELLING COMMUNITY

Jafet Andersson (Swedish Meteorological and Hydrological Institute (SMHI)), Berit Arheimer (SMHI), Hasnain Aslam (University of Tokyo), Gianpaolo Balsamo (ECMWF), Martyn P. Clark (University of Saskatchewan), Chris DeBeer (University of Saskatchewan), Mohamed Elshamy (Environment and Climate Change Canada (ECCC), Global Institute for Water Security (GIWS) (University of Saskatchewan)), Xing Fang (University of Saskatchewan), Riley Hales (Brigham Young University (BYU)), Shaun Harrigan (European Centre for Medium-range Weather Forecasts (ECMWF)), Rohini Kumar (Helmholtz Centre for Environmental Research – UFZ), Sujay Kumar (National Aeronautics and Space Administration (NASA)), Rosberg Jörgen (SMHI), Christopher Marsh (University of Saskatchewan), Jim Nelson (BYU), Henrik Madsen (DHI), John Pomeroy (University of Saskatchewan), Daniel Prinz (ECCC, GIWS (University of Saskatchewan)), Oldrich Rakovec (Helmholtz Centre for Environmental Research – UFZ), Robert Reinecke (Johannes Gutenberg University Mainz), Luis Samaniego (Helmholtz Centre for Environmental Research – UFZ), Hannes Müller Schmied (Goethe University Frankfurt, Senckenberg Leibniz Biodiversity and Climate Research Centre (SBIK-F), Frankfurt), Tricia Stadnyk (University of Calgary), Edwin H. Sutanudjaja (Utrecht University), Niko Wanders (Utrecht University), Albrecht Weerts (Deltares), Kosuke Yamamoto (Japan Aerospace Exploration Agency), Kei Yoshimura (University of Tokyo), and Xing Yuan (Nanjing University of Information Science and Technology), who contributed to the initial discussions, report preparation, global modelling and remotely sensed data, feedback and review.

GLOBAL DATA CENTRE AND EXTERNAL EXPERTS

Elie Gerges (International Groundwater Resources Assessment Centre (IGRAC)), Elisabeth Lictevout (IGRAC), Uli Looser (Global Runoff Data Centre (GRDC)), Arnaud Sterckx (IGRAC), and Matthias Zink (International Soil Moisture Network (ISMN)), who supported the preparation of the report. We also thank Anil Mishra (United Nations Educational, Scientific and Cultural Organization (UNESCO)) and Guy Reshef (Israel, Standing Committee on Hydrological Services) for their contribution to the preparatory workshop for this report.

CONTRIBUTORS AND CO-AUTHORS FOR SPECIFIC CHAPTERS

Groundwater: Elie Gerges (IGRAC), Elisabeth Lictevout (IGRAC) and Arnaud Sterckx (IGRAC), supported the preparation of the report and methodology.

Evapotranspiration and Soil moisture: Sujay Kumar (NASA) and Wanshu Nie (NASA).

Terrestrial water storage: Andreas Guentner (German Research Centre for Geosciences (GFZ)), who provided the terrestrial water storage data, which forms an important part of the present report.

Snow cover and glaciers: Leandro Cara (Instituto Argentino de Nivología, Glaciología y Ciencias Ambientales, Mendoza, Argentina), Duncan Christie (Center for Climate and Resilience Research, Santiago, Chile), Joel Fiddes (Institute for Snow and Avalanche Research, Davos, Switzerland), René Garreaud (Center for Climate and Resilience Research, Santiago, Chile), Simon Gascoïn (Centre d'études spatiales de la biosphère (Cesbio), France), George Kordzakhia (Georgian HydroMet Service), Mariano Masiokas (Instituto Argentino de Nivología, Glaciología y Ciencias Ambientales, Mendoza, Argentina), Lawrence Mudryk (ECCC), L. Shengelia (Georgian HydroMet Service), Genadi A. Tvauri (Georgian HydroMet Service), Ricardo Villalba (Instituto Argentino de Nivología, Glaciología y Ciencias Ambientales, Mendoza, Argentina), and Tandong Yao (Institute of Tibetan Plateau Research, China).



WMO SECRETARIAT LEAD AUTHORS

Sulagna Mishra (Scientific Officer), Stefan Uhlenbrook (Director Hydrology, Water and Cryosphere) and Rodica Nitu (Scientific Officer, Cryosphere chapter) who were also supported by hydrology colleagues of the Secretariat in producing and reviewing the report. Ryutaro Ikeda prepared the interactive web version of the report that can be found at <https://storymaps.arcgis.com/stories/8f5ecb9a58ec41e182675708caa58356>.

INDEPENDENT CONSULTANTS

Anastasia Lobanova and Iulii Didovets, carried out most of the scientific analysis to produce the results reported in the present report and contributed significantly to writing it.

BYU Civil & Construction
Engineering

Deltares



ECMWF

GFZ
Helmholtz Centre
POTSDAM



igrac
International Groundwater Resources Assessment Centre



SENCKENBERG
world of biodiversity

SMHI

UFZ HELMHOLTZ
Centre for Environmental Research



**UNIVERSITY OF
SASKATCHEWAN**

**Utrecht
University**

List of abbreviations

AWT	Asian Water Tower
DJF	December–January–February
ET	evapotranspiration
ENSO	El Niño–Southern Oscillation
ESA CCI	European Space Agency Climate Change Initiative
GHMS	global hydrological modelling system
GRACE	Gravity Recovery and Climate Experiment
GRanD	Global Reservoir and Dam
GRDC:	Global Runoff Data Centre
HydroSOS	Hydrological Status and Outlook System
IGRAC	International Groundwater Resources Assessment Centre
IOD	Indian Ocean Dipole
ISMN	International Soil Moisture Network
JJA	June–July–August
JRC	Joint Research Centre (European Commission)
MAM	March–April–May
MODIS	Moderate Resolution Imaging Spectroradiometer
NHMS	National Hydrological and Meteorological Service
SCA	snow-covered area
SDGs	Sustainable Development Goals
SON	September–October–November
SWE	snow water equivalent
TWS	terrestrial water storage
WHOS	WMO Hydrological Observing System

Executive summary



KEY IMPROVEMENTS IN THE 2022 REPORT

- **Inclusion of new hydrological cycle components:** The report was extended to include anomalies of groundwater levels, soil moisture, evapotranspiration, snow and ice, and reservoir inflows. Data were obtained from observed data sets, satellite remote sensing, and numerical modelling.
- **Expansion of observational data:** There was a substantial increase from 38 stations in the previous report to 273 stations in 2022. However, with data from only 14 countries, regions like Africa, the Middle East and Asia remain largely underrepresented. Also, more observations on key components of the hydrological cycle are needed for deriving trends and validation of models, for example, soil moisture, groundwater levels and evapotranspiration.
- **Enhanced spatial resolution:** The analysis now covers more than 1 000 river basins globally. Still, some areas, such as the United Kingdom, require further refining.

HYDROLOGICAL CONDITIONS AND SIGNIFICANT EVENTS OF 2022

- **River discharge and reservoir inflow patterns:** Over 50% of global catchment areas and reservoirs displayed deviations from normal conditions, of which a majority were drier than usual, aligning closely with 2021 data which also predominantly showed dry to normal conditions.
- **Soil moisture and evapotranspiration:** Throughout 2022, anomalies in soil moisture and evapotranspiration echoed the deviations in river discharge conditions; for example, Europe experienced increased evapotranspiration and decreased soil moisture during summer, conditioned by drought.
- **Droughts:** Severe droughts impacted regions including the United States, Horn of Africa, Europe, Middle East and La Plata basin. Europe's drought posed challenges in rivers like the Danube and Rhine and disrupted nuclear electricity production in France due the lack of cooling water. These areas also saw depleted inflows into reservoirs and decreased soil moisture and evapotranspiration levels.
- **Extreme weather in Asia and Oceania:** The Yangtze river basin in China faced a severe drought, while Pakistan's Indus river basin witnessed extreme floods. The disaster resulted in at least 1 700 fatalities, with 33 million people affected, and nearly 8 million people displaced. The total damage and economic losses were estimated at US\$ 30 billion. Eastern Australia's Murray–Darling river basin, New Zealand, and the Winnipeg basin in Canada experienced several flood events.
- **Africa's contrasting hydrological situations:** While the Horn of Africa dealt with a severe drought affecting 21 million people's food security, areas like the Niger basin and coastal areas of South Africa saw above-average discharge and major flood events.
- **Cryosphere:** In 2022, the snow cover in the Alps remained significantly below the 30-year average, affecting discharge of the major European rivers. The Andes saw declining winter snow, with the lowest amount in 2021 and some recovery in 2022, impacting water supplies in Chile and Argentina. Observations of Georgia's glaciers, especially the Shkhara, revealed a doubling of melting rates over recent years. Significant glacial melting was observed in the Asian Water Tower, along with changing river run-offs in the Indus, Amu Darya, Yangtze and Yellow river basins, highlighting the deepening influence of climate change on regional water resources.

REPORT IMPLICATIONS AND FUTURE OUTLOOK

With the inclusion of new components, based on increased observational data and modelling results, the present report offers a comprehensive view of the status of global water resources. The goal remains to amplify observational data and further the involvement of countries for a better understanding of water cycle dynamics. It is hoped that future reports will work with even more in situ data, aided by initiatives like WMO's Hydrological Status and Outlook System (HydroSOS).

Foreword



The publication of WMO's State of Global Water Resources report for 2022 follows the success of the pilot report launched last year in response to calls made at various global forums for an independent and consistent assessment of global water resources to guide policy discussions. The report received tremendous attention and validation from WMO Members, the international community, partners and media, and WMO is committed to continuing to publish this report annually. The publication of the State of Global Water Resources report is one of three Water

Action Agenda commitments made by WMO at the UN 2023 Water Conference. This WMO flagship report gives a concise presentation of the status of water resources in large basins in comparison to the long-term average, for various variables characterizing the water cycle.

In comparison to the first edition, which reported conditions of streamflow, terrestrial water storage and selected cryosphere parameters only, the present WMO *State of Global Water Resources 2022* report has been extended to include variables describing groundwater, evapotranspiration, soil moisture and reservoirs, along with an overview of the major extreme hydrological disasters around the globe in 2022. The 2022 report has also been improved compared to the pilot report in terms of spatial disaggregation of the basins thanks to the contributions from WMO Members and other experts with respect to in situ and modelled data. I would also like to note increased engagement in the various rounds of review of the content.

Along with in situ data, global hydrological and land surface modelling systems and remotely sensed data were largely used in preparing the 2022 report to achieve maximum global coverage and bridge data gaps, and we observed a good correlation between modelled and observed results. Although we have seen a substantial increase in data sharing and engagement from Members in the process this year, at a global scale we are still far from our goal of having this report globally uniformly based on hydrological observations. This can only be achieved through investments in monitoring and data sharing (in accordance with the WMO Unified Data Policy). Once the WMO Hydrological Status and Outlook System (HydroSOS), which is currently being implemented at various scales, is fully operational, the annual State of Global Water Resources report can be produced as a direct output of this system.

The present report demonstrates the practical utility of an annual global synthesis of the state of global water resources, and policy guidance such a synthesis can provide. This holds great importance, especially for making decisions at a large scale and for developing related policies. Furthermore, the report can play a crucial role in informing and directing discussions among different governments and water users regarding water resource dynamics and sustainable allocation and planning.

Our objective is to inform world leaders, policymakers, National Hydrological and Meteorological Services, experts and the general public about the current state of global water resources in comparison to previous years. The report also emphasizes the effects of weather and



climate events on the various aspects of the water cycle. In this light, the report acts as a vital stride towards fulfilling the United Nations Secretary-General's vision of establishing a comprehensive early warning system for all in the coming years, as well as contributing to achievement of the Sustainable Development Goals (SDGs) and other global objectives related to water and climate.

I congratulate the steering committee members and the lead authors for compiling the 2022 report. Likewise, I would like to express my sincere thanks to all the experts and contributors, particularly WMO Member National Hydrological and Meteorological Services, global data centres, global hydrological modelling community members, and supporting organizations – the National Aeronautics and Space Administration (NASA) and the German Research Centre for Geosciences (GFZ) – for their continued support.

(Prof. Petteri Taalas)
Secretary-General

Introduction

The State of Global Water Resources report series offers a comprehensive and consistent overview of water resources worldwide, highlighting the influence of climatic, environmental and societal changes on the hydrological variables. The 2022 edition of the State of Global Water Resources Report marks the second report in the annual series, following the successful pilot edition for 2021 launched in 2022. The first edition of the report was well received and led to increased participation from WMO Member States and Territories, National Hydrological and Meteorological Services, and other organizations, including members of the global hydrological modelling community, in the preparation of the 2022 report. Its impact was further amplified by substantial engagement from external stakeholders and the general public, as well as wide media coverage.

With global coverage, the report presents crucial hydrological indicators, including, for example, changes in river discharge, reservoir inflow, groundwater levels and others, helping to identify annual patterns and hydrological hotspots around the globe. By analysing various aspects such as distribution and quantity across time and space, the report serves as a valuable resource for policymakers, water managers and disaster risk reduction efforts, fostering a better understanding of global freshwater trends. In the future, the report will also provide a historical perspective on the state of global water resources, which will help to identify and understand regional and global trends.

The report contributes directly to achieving SDG 6: Clean Water and Sanitation, and other SDGs that are related to water by providing essential data to design targeted interventions for sustainable water resources management and address water scarcity/overabundance and quality issues. By enhancing understanding of climate-related impacts on water systems, the report supports SDG 13: Climate Action, informing strategies to align water resources management with climate change mitigation. The report also enables inter-annual comparisons to differentiate short-term effects from long-term trends in the factors driving water distribution patterns. The report’s collection and dissemination of observed and modelled data sets on global water resources stress the significance of transparent data sharing, reinforcing SDG 17:

Partnerships for the Goals, by enhancing global partnerships and cooperation, and enabling more informed, collaborative efforts toward sustainable water and environmental management. The report provides an overview of the status of data availability and encourages data sharing, which is crucial for developing meaningful products for the United Nations Early Warnings for All initiative. The graphical global summaries of various hydrological components help in identifying the hotspots to inform planning, preparedness and management of disasters.

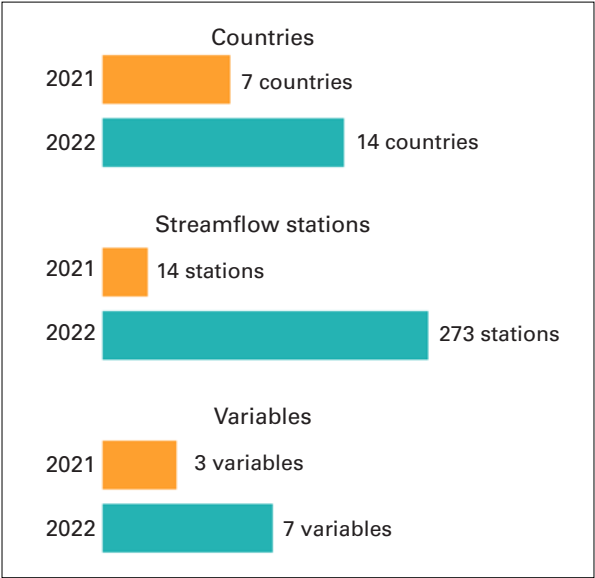


Figure 1. Comparison of the number of countries, number of stations with observed river discharge data (both quality-controlled and not) and variables available for the reports on the years 2021 and 2022

Figure 1 provides an overview of the number of countries, number of stations with observed river discharge data (both quality-controlled and not) and variables available for the reports on the years 2021 and 2022. In addition to the chapters on river discharge, terrestrial water storage, high-impact events and the cryosphere, the 2022 edition of the report contains several new chapters that portray the state of crucial hydrological variables, in particular, chapters on groundwater, inflow into reservoirs, soil moisture and evapotranspiration.



The 2022 report is organized into the following chapters: the main results are distributed into chapters on [River discharge](#), [Reservoirs](#), [Groundwater levels](#), [Soil moisture](#), [Evapotranspiration](#) and [Terrestrial water storage](#), each one showing either the global or the regional perspectives. The chapter on [Snow cover and glaciers](#) captures changes in the cryosphere, focusing on Central Asia, Central Europe and the subtropical Andes. The chapter on [High-impact hydrological events](#) provides a global overview of the major hydrological events that occurred in 2022. The [Synthesis](#) provides a summary of the major findings observed in the state of global water resources during calendar year 2022.

Access to observational in situ data plays a crucial role in assessing water resource conditions and validating modelling tools. In the current report, there has been a notable increase in observational river discharge data obtained from countries, with the number of stations reporting observed river discharge rising from 38 in the previous year to 273. However, in situ river discharge data from only 14 countries were available for this report, and regions like Africa, the Middle East and Asia are notably underrepresented due to lack of either observational data availability or data sharing.

Similarly, the modelled soil moisture data could not be validated with in situ observations in this year's edition due to lack of observational data at hand. At present, the International Soil Moisture Network (ISMN) collects observed soil moisture data mostly from scientific networks and not from nationally coordinated monitoring activities. Despite the fact that the number of contributing stations is increasing, there is an urgent need for more support from WMO Member States and Territories to build up national soil moisture databases, which should be connected to ISMN.

Enhancing data sharing and engagement from WMO Member States and Territories in future editions of the report will advance our understanding of hydrological processes in these regions, benefitting policymakers, water resource managers, water users and the general public, and providing better validation of models in these areas.

DATA SOURCES AND ANOMALY CALCULATION

For each of the variables presented in the chapters, the anomaly¹ was calculated by comparing the state in the year 2022 to the annual long-term means obtained from the historical period,² as described in Box 1.

Box 1

The annual mean of a hydrological variable (for example, river discharge, inflow into reservoirs) for a defined reference of modelled or observed data was calculated for each year. The ranking of Q in 2022 falls under categories based on the following definition:

much below normal:	$Q_{2022} \leq 10\text{th percentile}$
below normal:	$10\text{th percentile} < Q_{2022} < 25\text{th percentile}$
normal: ³	$25\text{th percentile} \leq Q_{2022} \leq 75\text{th percentile}$
above normal:	$75\text{th percentile} < Q_{2022} < 90\text{th percentile}$
much above normal:	$Q_{2022} \geq 90\text{th percentile}$

Note that while the reference period for the data varied for the different variables (30 years (1991–2020) for river discharge, 10 years (2013–2022) for groundwater and 19 years (2002–2020) for terrestrial water storage) based on data availability, the classification of the ranking remained the same.⁴



[Annex 1](#) contains: (a) further details on the methods, including an overview of the data sources and global hydrological models used in the analysis; (b) the definitions of the indicators used in the report; (c) additional results. [Annex 2](#) provides exhaustive information on the methods and data sources used in the [Groundwater levels](#) chapter.

The data used in the report were gathered from various sources (refer to Box 2 and [Annex 1](#)), including National Hydrological and Meteorological Services, Earth observations, and the global modelling community, ensuring a robust, spatially consistent and comprehensive analysis. The [River discharge](#) chapter is based on modelled and observed data. The latter, where possible, were also used to validate the modelled trends.

Box 2

Data sources 2022

- *Observed river discharge data:* National Hydrological and Meteorological Services (NHMSs) of countries and the Global Runoff Database (GRDC).^{5,6}
- *Simulated river discharge data:* eleven global hydrological modelling systems (GHMSs) (see the [River discharge](#) chapter for the full list of models).
- *Inflow into selected reservoirs globally:* Wflow_sbm,⁷ CaMa-Flood⁸ and WWH⁹ models.
- *Groundwater data:* International Groundwater Resources Assessment Centre (IGRAC) for the selection of 10 countries.
- *Soil moisture and evapotranspiration:* Global water cycle reanalysis product NASA-LISF-Noah MP.^{10,11,12}
- *Global terrestrial water storage (TWS):* the GRACE project.^{13,14}
- *Glaciers:* WMO Member States and Territories and external experts.
- *High-impact events:* open data sources, such as the EM-DAT database,¹⁵ ReliefWeb, contributions of countries to WMO State of the Global Climate Report and others.

THE BACKDROP: OVERVIEW OF CLIMATIC CONDITIONS IN 2022

Two major climate patterns, the El Niño–Southern Oscillation (ENSO) and the Indian Ocean Dipole (IOD), played key roles in 2022’s climate dynamics and rainfall patterns globally and regionally.¹⁶ ENSO, a key driver of climate variability globally, exhibited La Niña conditions for the third consecutive year – a rare occurrence known as a “triple-dip” La Niña, which occurred only three times in the last half-century. This resulted in certain regions experiencing typical La Niña-induced weather and climate extremes, like dry conditions in Patagonia and South-west North America, while others like South-east Asia saw intensified monsoon rains. East Africa’s drought, aggravated by both La Niña and the negative phase of IOD, had dire humanitarian consequences. Although it has a general cooling effect, La Niña led to warmer conditions in some regions, such as New Zealand, which reported its warmest year on record. Despite the ongoing La Niña conditions, the global mean temperature was 1.15 [1.02–1.28] °C above the 1850–1900 average, making 2022 the fifth or sixth warmest year on record.

IOD’s influence was also pronounced. Its negative phase, coupled with La Niña, contributed to Australia’s exceptionally wet conditions, especially in New South Wales and Victoria. This negative IOD phase, however, transitioned to neutral by the beginning of the austral summer.



Both these climate patterns, ENSO and IOD, heavily influenced the precipitation anomalies observed globally in 2022. North-east Asia, South-east Asia, certain North American and South American zones, Eastern Europe, and some parts of Africa, New Zealand and Australia saw above-average precipitation. In contrast, large parts of Europe, North-west Africa, Central Asia, Eastern Africa, and areas in the Americas experienced rainfall shortages.

The Indian Monsoon arrived early and receded late, leading to above-average rainfall across the Indian subcontinent. This rainfall extended unusually far westward into Pakistan, causing significant flooding. The West African Monsoon, meanwhile, was delayed but eventually brought rainfall volumes close to long-term norms, excluding some coastal areas.

River discharge

The 2022 edition of the State of Global Water Resources report adopts the Hydrobasins level 4 delineation,¹⁷ bringing the total number of river basins to approximately 1 000 basins (after applying a minimum area threshold of 10 000 sq km) around the globe (see [Figure A1](#) of Annex 1).

The river discharge analysis in the 2022 edition of the report, similar to the 2021 pilot edition, is based on in situ data received from WMO Member States and Territories supplemented with substantial contributions from the global hydrological modelling and Earth observation community. The 11 global hydrological modelling systems (GHMSs) listed below were used for this year's report. Eight GHMSs were used for river discharge calculations. Four GHMSs also provided simulations for other variables like soil moisture, evapotranspiration and inflow to reservoirs:

- The CaMa-Flood with Dam model^{18,19} (used for river discharge and inflow to reservoirs);
- The Conjunctive Surface–Subsurface Process, version 2 (CSSPv2) model²⁰ (employed only for river discharge intercomparison);
- The Wflow_sbm model^{21,22,23} (used for inflow to reservoirs, and river discharge comparisons for Europe);
- The DHI-GHM²⁴ (used for river discharge calculations);
- The Copernicus Emergency Management Service Global Flood Awareness System (GloFAS)^{25,26} (used for river discharge calculations);
- The European Centre for Medium-Range Weather Forecasts (ECMWF) Land Surface Modelling System (ECLand)²⁷ (used for river discharge calculations);
- The Mesoscale Hydrologic Model (mHM)^{28,29,30} (used for river discharge calculations);
- The NASA-LISF-Noah MP model^{31,32} (employed only for river discharge model intercomparison, due to shorter historical simulation period and used for calculating trends for soil moisture and evapotranspiration);
- Today's Earth – Global (TEJRA55)^{33,34} (used for river discharge calculations);
- The WaterGAP 2.2e model^{35,36} (used for river discharge calculations);
- The World-Wide HYPE (WWH) model, v1.3.9³⁷ (used for river discharge, and inflow to reservoirs).

For more information about the models, the input data used and other details, please refer to the [Global hydrological modelling systems](#) section of Annex 1.

The volume of observational data for the year 2022 collected from the National Hydrological and Meteorological Services (NHMSs) and the Global Runoff Data Centre (GRDC) database^{38,39} has seen a substantial increase since the previous version of the report (Figure 1). At the time of preparation of this report, observed daily river discharge data (covering the entire year 2022) were available at 273 stations, in comparison to 38 stations used in the 2021



water report (Figure 2 and Figure A2 of Annex 1). Most of the stations are located in North America (60%), while South America, Australia and Europe each have a share ranging from 12% to 14%. The smallest proportion of available stations is found in Africa and Asia, collectively accounting for around 1%.

In total, for this year’s report there were nearly 500 stations with observed data for the year 2022 available. However, the analysis is based on the 273 stations that had data for the whole year. Only stations with at least 345 days of data points for 2022 and covering a historical period of at least 20 years (2001–2020) were selected for the analysis (see Figure A2 of Annex 1 for the gauge locations for all available data, and data used in the report).

The mean annual river discharge data for 2022 obtained from GHMSs and observation were compared with the historical values over the years 1991–2020 and then classified as normal, above normal, much above normal, below normal or much below normal with respect to historic values (refer to the Methods section in Annex 1 for more details). There was a minor revision in the definition of hydrological normal from the 2021 report (details on the definition of normals can be found in Box 1).

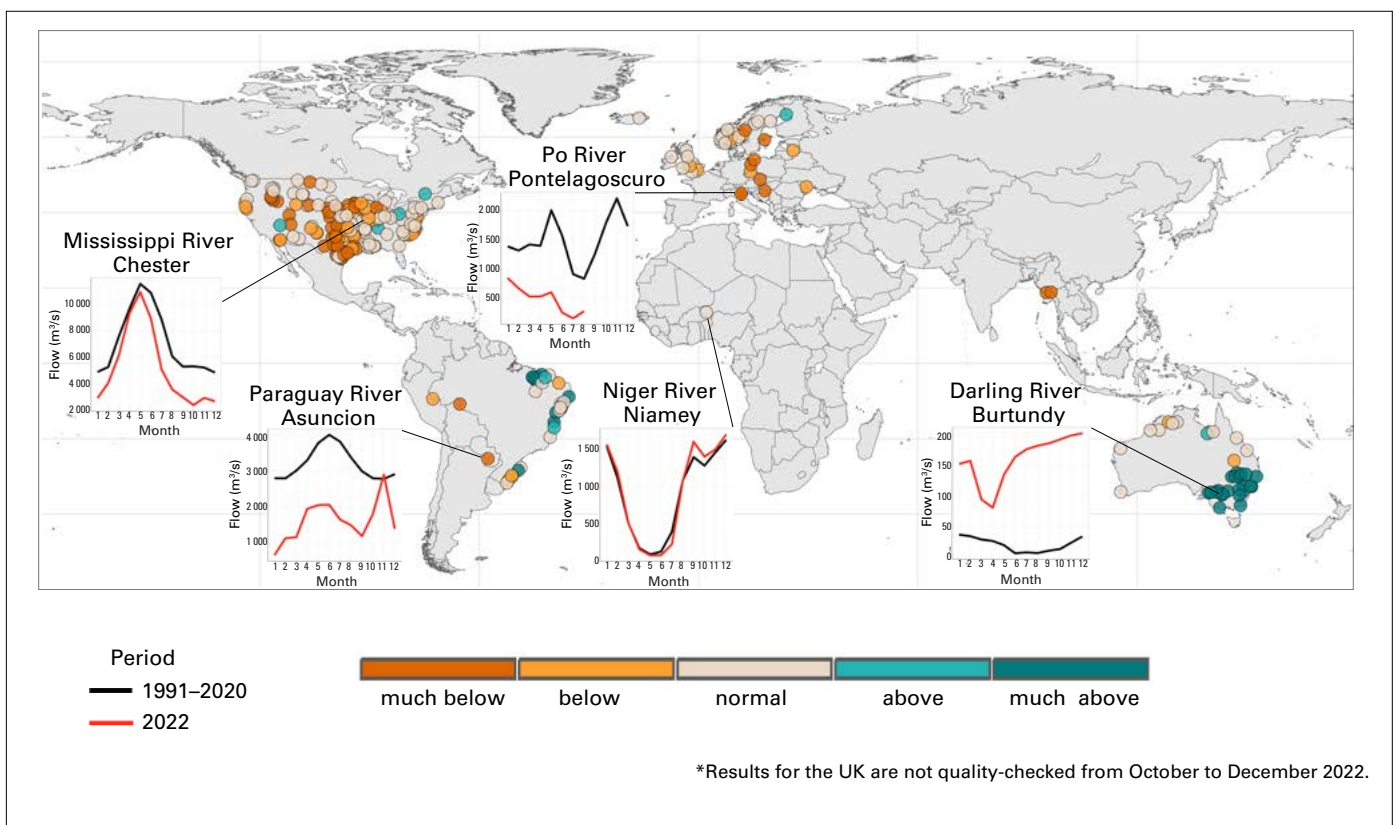


Figure 2. Observed mean river discharge for the year 2022 compared to the period 1991–2020 (for stations with a minimum of 20 years of data availability (2001–2020)); the dots are placed at the gauging station location (that is, the gauged basin outlet). The results presented here were derived from the observed river discharge data, which were obtained from NHMSs and the GRDC database. The results were also used to validate the simulated GHMS results in Figure A6 of Annex 1, where the reference period was adjusted to match the available in situ data. Results for the Po River were obtained from Zanchetin⁴⁰ and Montanari et al.⁴¹

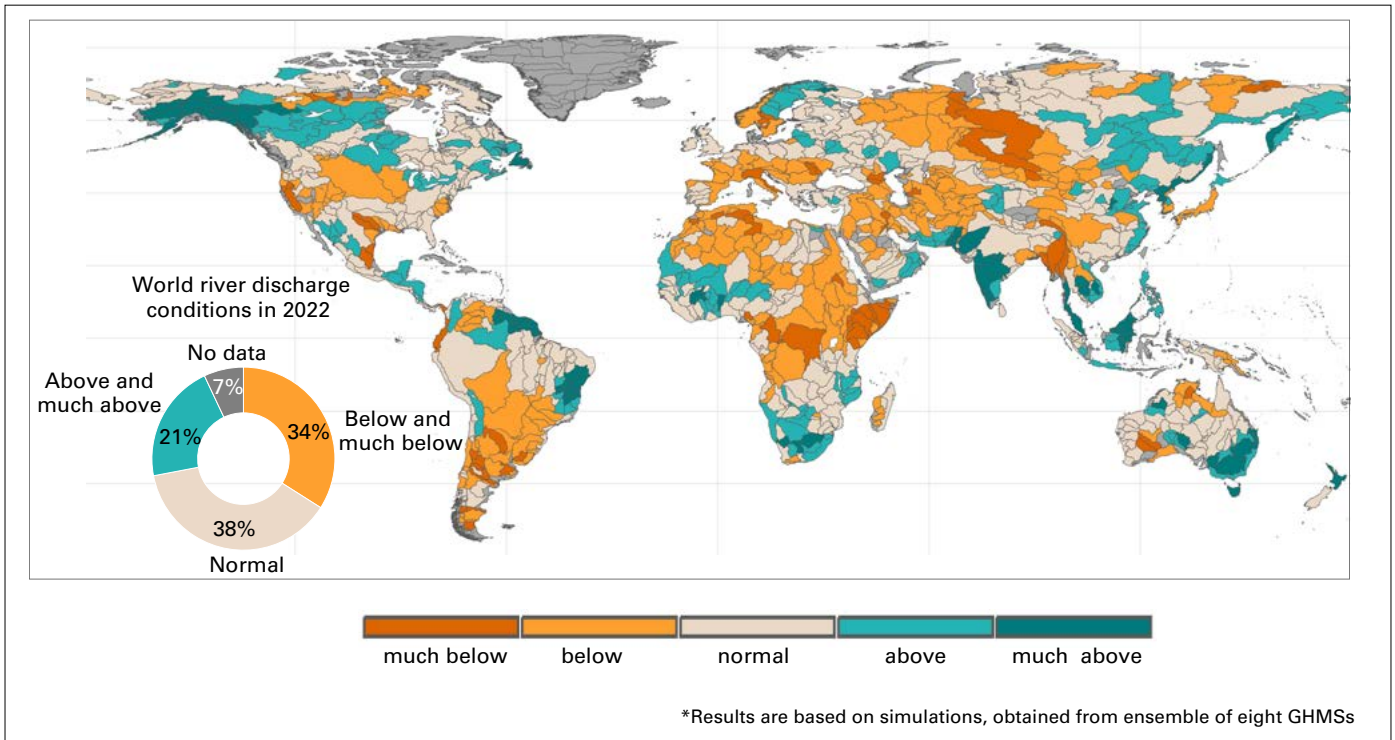


Figure 3. Mean river discharge for the year 2022 compared to the period 1991–2020 (for basins larger than 10 000 km²). The results presented here were derived from the modelled river discharge data, which were obtained from an ensemble of eight GHMS simulations (see [Methods](#) in Annex 1). Inset (bottom left) shows the percentage distribution of the modelled catchment area under the given conditions. Dark gray areas indicate missing river discharge data. The results were validated against hydrological observations wherever available (see [Figure A6](#) of Annex 1).

Figure 3 presents the anomaly in river discharge for the year 2022 compared to the selected historical period (1991–2020) calculated based on ensemble results from the hydrological models (see [Annex 1](#) for details on the method of calculations). In cases where observational data were available, they were used to validate the modelled results. A detailed presentation of the validation is provided in [Figure A6](#) of Annex 1.

Validation of modelled results showed overall good agreement (>60% of basins) between observed and simulated anomalies for the year 2022, particularly in Myanmar, Australia, the eastern and central United States, Central Europe, and the upper La Plata basin. At the same time modelled anomalies based on multi-model mean disagree with observations in parts of the Niger basin, the northern Amazon and the coastal areas of Brazil, the northern United States, the United Kingdom and Northern Europe.

Box 3

For this year’s report, a total of 11 different GHMSs were used in the modelling analysis. [Annex 1](#) provides details on each of the GHMSs used, together with information on their set-up, their calibration with historical data and how simulations for 2022 were produced. It also outlines potential sources of uncertainty associated with the modelling framework applied. In basins for which observed river discharge data were available, the trends simulated by the GHMSs were validated.⁴²



As shown in Figure 3 (anomalies in river discharge in 2022), in more than 50% of global catchment area river discharge exhibited deviations from near-normal conditions; it was predominantly lower than normal, with a smaller proportion of basins exhibiting above-normal and much-above-normal conditions.⁴³

In South America, significant portions of Argentina, Paraguay, Uruguay, Chile and southern Brazil recorded below-normal to much-below-normal river discharge. In the La Plata river basin, drought conditions established since 2020 persisted into 2022⁴⁴ and resulted in impacts on agriculture, inland water navigation, energy production and water supply. Lower-than-normal precipitation totals continued to late September 2022, which exacerbated the already low river discharge.

In North America, the central and western regions of the United States showed below-normal to normal river discharge records; record low levels were observed in the Mississippi Basin in 2022, affecting barge movements along its waterway,⁴⁵ as also indicated by the observed reservoir inflows (Figure 4). The drought conditions in this area, which began in 2019, continued through 2022. In contrast, the Yukon (Alaska) and Mackenzie (Canada) river basins had much-above-normal and above-normal river discharge, respectively. Across the Winnipeg river basin the discharge was above average in 2022. More than half of the gauged tributaries across the basin set new all-time flow records and flooding lasted for months, causing extensive damage and states of emergency in the provinces of Ontario and Manitoba (Canada) and the state of Minnesota (United States).⁴⁶

The discharge conditions in the Horn of Africa were much below normal in 2022. The area continued to suffer the longest and the most severe drought event on record in 2022,⁴⁷ which started in 2020, with much-below-normal annual discharge conditions. The extraordinary run of four successive dry rainfall seasons⁴⁸ in the Horn of Africa, which may be partially attributed to human-driven warming,^{49,50} sea surface temperatures in the Indian Ocean and La Niña, was compounded by the arrival of a fifth rainy season in 2022 marked by scarce rainfall.⁵¹

The Congo River and the entire catchment of the Nile River in Central Africa exhibited reduced river discharge. In contrast, the Niger basin, and almost the entire territory of South Africa, including the Orange river basin, showed above-normal river discharge. The Niger basin and the east coast of South Africa (KwaZulu-Natal and Eastern Cape provinces) suffered major flood events in 2022.

Throughout Central and Western Europe, river discharge levels were below normal, as a result of extreme heat and drought in 2022.⁵² Basins draining the Alps and Carpathians into rivers such as the Danube, Loire, Rhine and Po, exhibited significantly low levels during the summer of 2022. Rivers in southern Norway and southern Sweden were also affected and exhibited below-normal discharge conditions.

The entire territories of the Islamic Republic of Iran, Iraq, Syrian Arab Republic, Afghanistan and Myanmar, and the Amu Darya and Syr Darya basins in Central Asia saw below-normal and much-below-normal discharge conditions in 2022. Also, in the southern part of China, the Yangtze River, affected by drought and prolonged heat, reached record-low water levels⁵³ affecting almost 5 million people.⁵⁴ India, and especially Pakistan, were hit by severe flooding in 2022 caused by very high precipitation concentrated during the monsoon period. The Godavari and Krishna Rivers in the southern part of India exhibited much-above-normal river



discharge in 2022. In Pakistan, the lower part of the Indus basin exhibited much-above-normal river discharge in 2022. Details of socioeconomic losses caused by the major hydrological disasters are listed in [High-impact hydrological events](#).

Eastern Australia, particularly the Murray–Darling river basin, exhibited above-normal river discharge conditions. In fact, several flood events occurred in Australia in 2022. Malaysia, Indonesia and the Philippines saw above-normal river discharge conditions, as well as the North Island of New Zealand. The river discharge conditions of the South Island of New Zealand remained near normal.

Reservoirs

This chapter presents anomalies in the water inflow into a selection of reservoirs around the globe in the year 2022. The inflow data were obtained from three sources that comprise satellite-based⁵⁵ and GHMS products, namely the Wflow_sbm,⁵⁶ CaMa-Flood with Dam^{57,58} and WWH models.⁵⁹ All available reservoirs from these sources were included for analysis and were identified by their GRanD id.⁶⁰ Daily inflows into the selected GRanD reservoirs were computed from the three models for the historical period between 1991 and 2020 and for the year 2022, and the 2022 inflows were ranked against the historical period following the same method as for river discharge (refer to Box 1 for details). Water inflow into the reservoirs was selected as an indicator due to its lower dependency on water resources management strategies, such as reservoir operations. The size of the dots corresponds to the maximum storage volume of the reservoirs. The observed monthly reservoir surface area anomalies in the year 2022 are presented in [Figure A7](#) of Annex 1.

Following the general trend in river discharge around the globe in 2022, more than 60% of reservoirs under consideration received either more or less than normal water inflow. Similar hotspots were exhibited in several regions. In particular, reservoirs located in Central Asia, the Middle East, Central Africa and Central America, along with all areas across Southern and Central Europe, the United Kingdom, Iceland and the southern part of Scandinavia experienced water inflow rates lower than normal throughout the year 2022 (Figure 4).

The impact of drought conditions across Europe was clearly observed in the reduced inflow to the majority of reservoirs, with the exception of far northern catchments in Norway and Sweden, which received above-normal inflow.

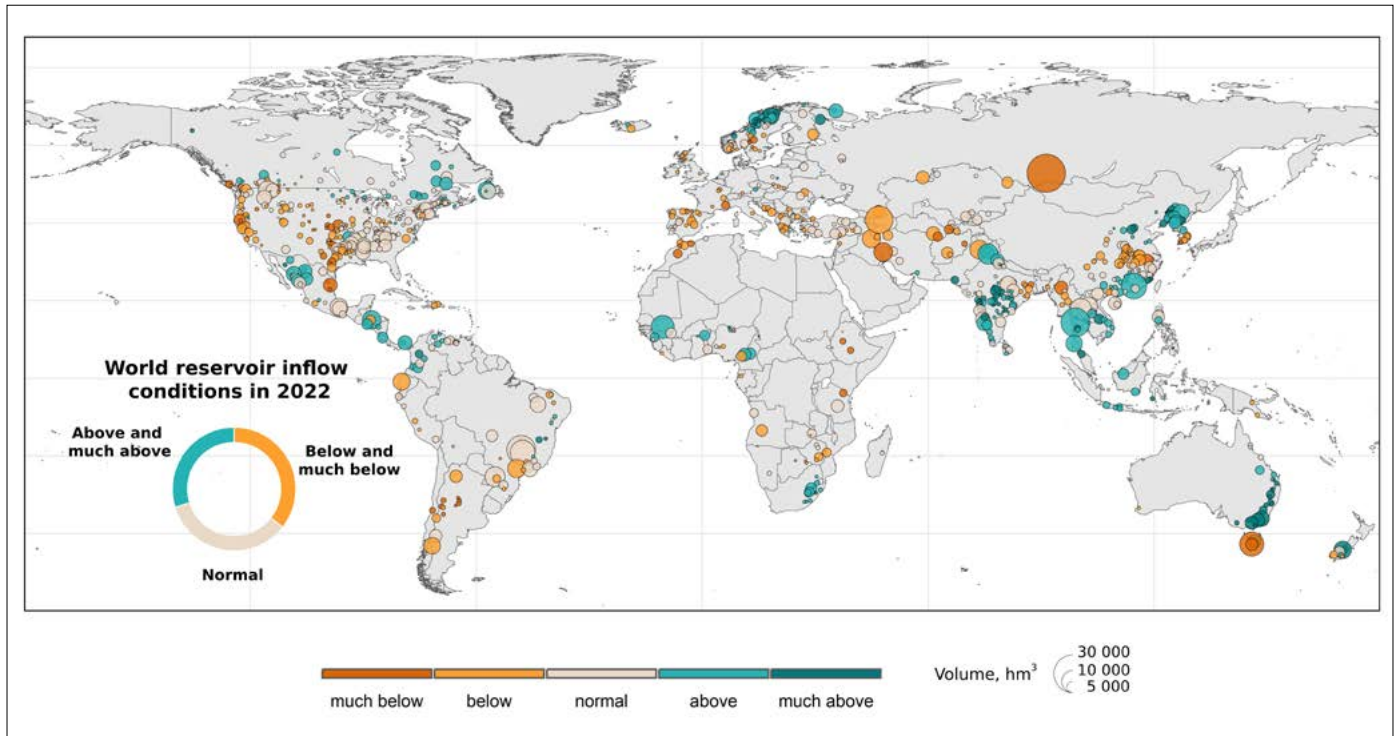


Figure 4. Anomaly in the mean annual inflow into selected reservoirs in 2022 as ranked with respect to the historical period 1991–2020. The results presented here were derived from the modelled reservoir operations data from two GHMSs and one hybrid satellite-based and modelling product (see [Table A2](#) of Annex 1 for more information). Inset (bottom left) shows the numbers of reservoirs under the given conditions.



In eastern China, specifically within the Yangtze river basin, reservoirs received notably less inflow than typically expected.

Reservoirs near the south-eastern coast of Australia and on the South Island of New Zealand experienced above-normal inflows.⁶¹

Following the notably high river discharge conditions and dramatic flood events in 2022, reservoirs in India and Pakistan received above-normal inflow.

Groundwater levels

This section presents a first attempt at reporting on the quantitative status of aquifers (or other reporting units that are relevant for the management of groundwater resources), based on groundwater level monitoring data received from national groundwater monitoring networks. The methodology consists of compiling groundwater-level hydrographs in each aquifer or reporting unit. The quantitative status of these units is assessed with two indicators that complement each other: (i) the rank of the mean groundwater level in 2022 as compared with previous years, and (ii) the multi-annual trend in groundwater levels. The methodology has been piloted in 10 countries, where data from the national groundwater monitoring networks were available, using a period of record of 10 years (2013–2022). In total, 8 246 wells were selected for the analysis. The relatively short period of record is a limiting factor for the interpretation of the results. So is the inadequacy of some reporting units, typically the units that are very large or heterogeneous.

These two indicators have been calculated for a selection of countries, for demonstration purposes. Therefore, the results shown in this section should not be used to make exhaustive conclusions on the state of groundwater resources in these countries in 2022. The objective is instead to illustrate the feasibility and the added value of such a reporting strategy, and to encourage the participation of WMO Member States and Territories in the report's next edition. A complete description of the methodology is available in [Annex 2](#), which also discusses the current limitations and the way forward and steps needed to apply the methods at the global scale.

Figure 5 shows the ranking of mean groundwater levels in 2022 compared to the previous years over the period (2013–2022). Figure 6 shows whether the linear trend of groundwater level has been rising, stable or declining, over the same period of 2013–2022. The maps also indicate the reporting units where no data points were available or selected (due to incomplete time series), and the units where the density of data points was deemed insufficient (<1/5 000 km²).

The preliminary results shown in Figures 5 and 6 are consistent with existing information about the state of groundwater in several regions. For instance, groundwater depletion in north-central Chile seems to be adequately reflected.⁶² In Brazil, the trends show a decline of groundwater levels in the Guarani aquifer towards the headwaters of the Parana and Paraguay Rivers, where most of the aquifer's exploitation occurs.⁶³ In Australia, the results capture the long-term groundwater decline observed in the south-west part of Western Australia.⁶⁴ In South Africa, the trends calculated in the Limpopo province and in the southern part of the country are in overall agreement with the groundwater level maps produced by the Department of Water and Sanitation.⁶⁵ In France, groundwater levels in 2022 were predominantly categorized as below normal, which correlates with the deficits of precipitation that occurred during the extreme heatwave and drought event in Europe in the summer of 2022.⁶⁶

On the other hand, some regions stand out because the preliminary results seem to not fully agree with existing information about the state of groundwater. A good example is the High Plains aquifer in the United States. Results indicate that groundwater levels were stable for 2013–2022; however, the water level in this aquifer has been declining for decades.⁶⁷ In preparing the next edition of the report, early engagement with national experts will be instrumental to carefully select the reporting units and to get access to longer time-series, in order to consolidate the methodology and expand the geographical coverage.

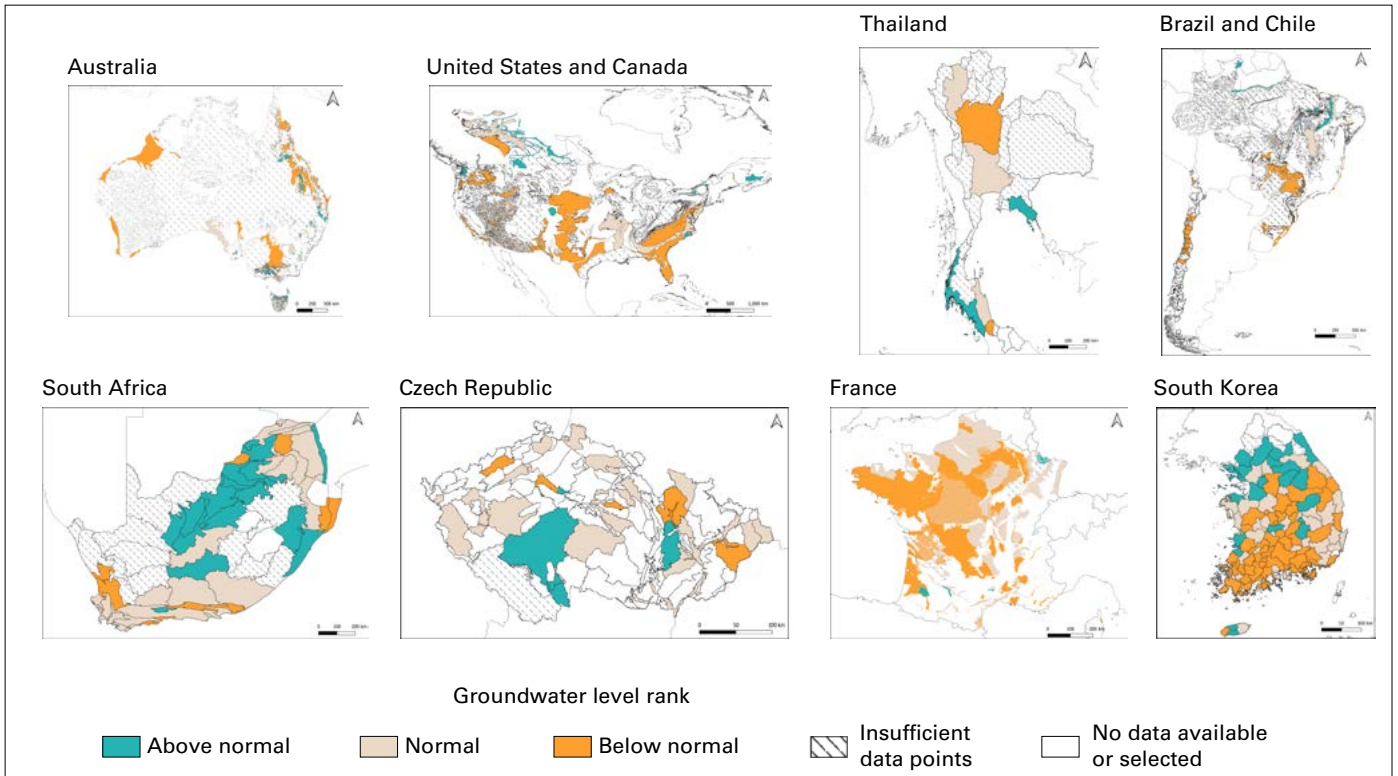


Figure 5. Mean groundwater levels in selected aquifers in 2022 ranked against the historical period 2013–2022 for selected countries. Reporting units that overlap are symbolized with a stripe pattern (for example in South Africa).

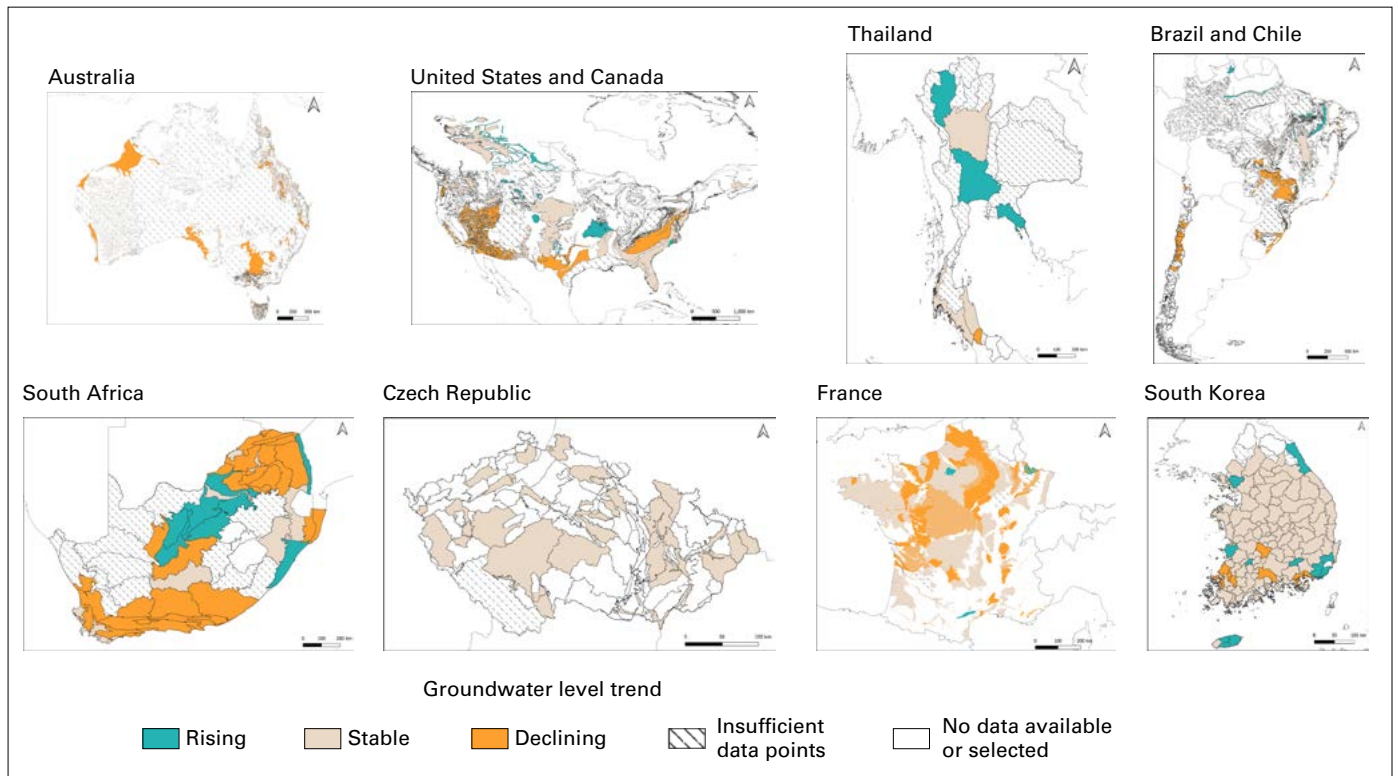


Figure 6. Groundwater level trends in selected aquifers for the period from 2013 to 2022 for selected countries. Reporting units that overlap are symbolized with a stripe pattern (for instance in South Africa).

Soil moisture

Surface soil moisture is one of the crucial variables for hydrological processes; it influences the exchange of water and energy fluxes at the land surface/atmosphere interface and impacts streamflow generation and vegetation development. Understanding soil moisture patterns is essential for sustainable water resources management.^{68,69} The anomaly in surface soil moisture (topsoil, 5 cm) in 2022 has been ranked relative to the historical period from 2003 to 2020 (Figure 7) on a monthly basis to understand near-surface soil moisture patterns.

The soil moisture and evapotranspiration (see the [Evapotranspiration](#) chapter) data sets were obtained from a global water cycle reanalysis product at 10 km spatial resolution.^{70,71}

The percentile algorithm was the same as used for river discharge and reservoir inflow (refer to Box 1 for details) and was used to determine the corresponding anomalies for 2022 based on the climatology of 2003–2020. The reanalysis product was created using the NASA Land Information System modelling framework⁷² by assimilating soil moisture data from the European Space Agency Climate Change Initiative (ESA CCI), leaf area index data from the Moderate Resolution Imaging Spectroradiometer (MODIS), and terrestrial water storage anomalies from the Gravity Recovery and Climate Experiment and the follow-on satellites (GRACE/GRACE-FO) using the Ensemble Kalman Filter approach following Kumar et al.⁷³

Unfortunately, soil moisture observations could not be used for this edition of the report because they are still sparsely distributed in space and time. The International Soil Moisture Network (ISMN) had only 42 locations with data of decent quality, temporal coverage and length of observations in 2022 out of 240 stations that had data for this year. ISMN is working on increasing this number significantly for the next report.

A positive soil moisture anomaly was recorded in 2022 during December–January and June–July in the Orange river basin and along South Africa’s east coast, which was affected by a flood in April 2022. In Pakistan, the Indus river basin, which experienced severe floods during the monsoon period, already showed much-above-normal soil moisture values in January, as well as in July and August following the flood event.

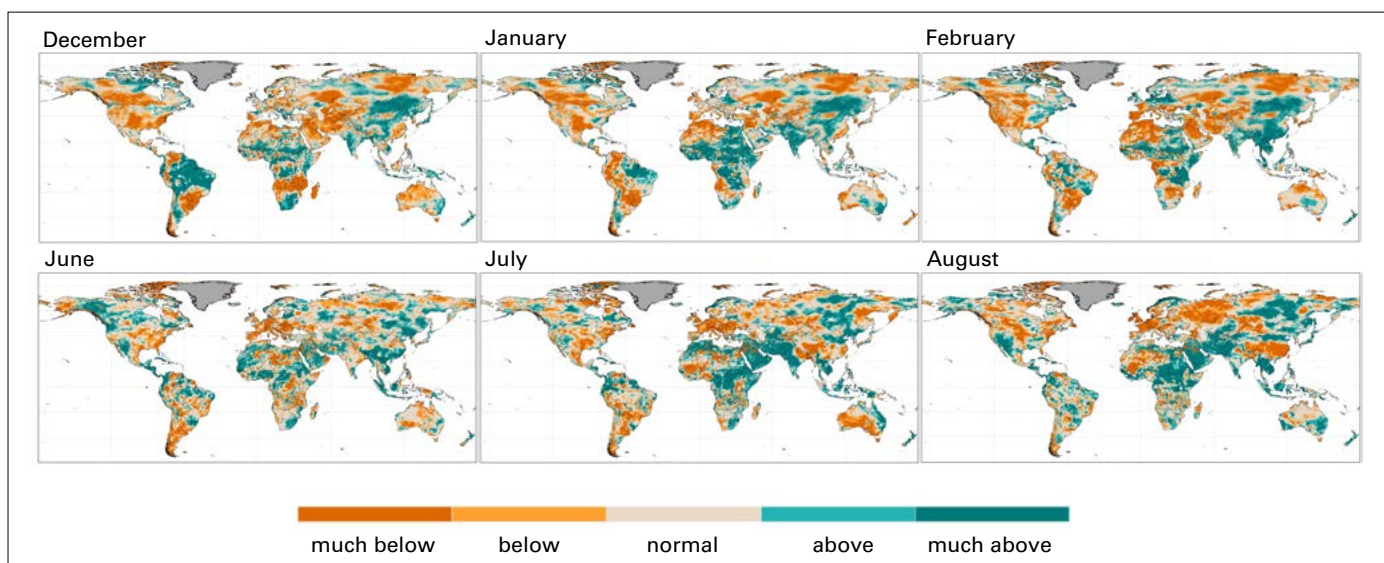


Figure 7. Monthly anomaly in surface soil moisture in 2022 (Dec. 2021–Feb. 2022 and Jun.–Aug. 2022) as ranked with respect to the historical period 2003–2020. The mask over Greenland from Global Land Ice Measurements from Space (GLIMS) has been applied.



The Yangtze river basin, which faced a 2022 summer heatwave, saw a gradual decrease in soil moisture over June–July, hitting a low in August 2022, when soil moisture values reached much-below-normal values.

In the Mississippi river basin, soil moisture remained below normal, even significantly so, for most of the year, likely due to the prevailing drought conditions. Annual mean soil moisture was much below normal over almost the entire territory of the United States.

In the La Plata basin, soil moisture conditions were substantially below normal during the December–February period, with a minor recovery in the headwaters in August, leading to above-normal soil moisture conditions in that month. However, despite this minor recovery in the headwaters of the basin, annual values remained significantly below normal in this region, especially in the lower part of the basin (see [Figure A8](#) of Annex 1).

Central and Eastern Europe, the United Kingdom, Ireland and parts of Scandinavia also witnessed below-normal soil moisture conditions during the summer months of June, July and August in the 2022 heatwave. Southern Europe and France experienced a soil moisture deficit as early as January–February 2022, further exacerbated by the summer heatwave. A continuous deficit in rainfall started in Central Europe in the winter of 2021/2022, and throughout the year, surface soil moisture reached the second lowest levels recorded in the past half-century.⁷⁴

Note that the results presented are based on the moisture content of the topsoil (5 cm), and thus represent a zone that quickly reacts to short-term atmospheric conditions. Deeper soil layers are controlled by medium- to long-term atmospheric conditions, and sometimes the connection to the groundwater, and may show different behaviour.

Evapotranspiration

Evapotranspiration (ET), which is one of the key elements in the hydrological cycle, refers to the process by which water is evaporated, encompassing evaporation from the soil or vegetation surface (including interception evaporation) and transpiration from plants. Elements influencing the rate of ET include the level of solar radiation, atmospheric vapour pressure, temperature, wind, soil moisture content and vegetation type. This process is responsible for a large part of the water loss from the soil during a crop's growth cycle and is critical for understanding the state of water resources. This chapter presents anomalies of actual ET at the global scale for four seasons in 2022. The rates of actual ET are controlled by the amount of water that is available (which is dependent on the initial hydrological conditions in the basin) in addition to the meteorological forcing.

The soil moisture (see [Soil moisture](#) chapter) and ET data sets are obtained from a global water cycle reanalysis product at 10 km spatial resolution,⁷⁵ as described in the [Soil moisture](#) chapter. The ET data are produced by the Noah-MP land surface model and refer to the sum of three components: soil evaporation, transpiration from vegetation and canopy interception evaporation. All reported ET values refer to the actual ET.

Figure 8 provides the seasonal anomaly in ET in 2022 as ranked with respect to the historical period 2003–2020.

Figures with annual average anomalies in both soil moisture and ET are included in [Annex 1](#).

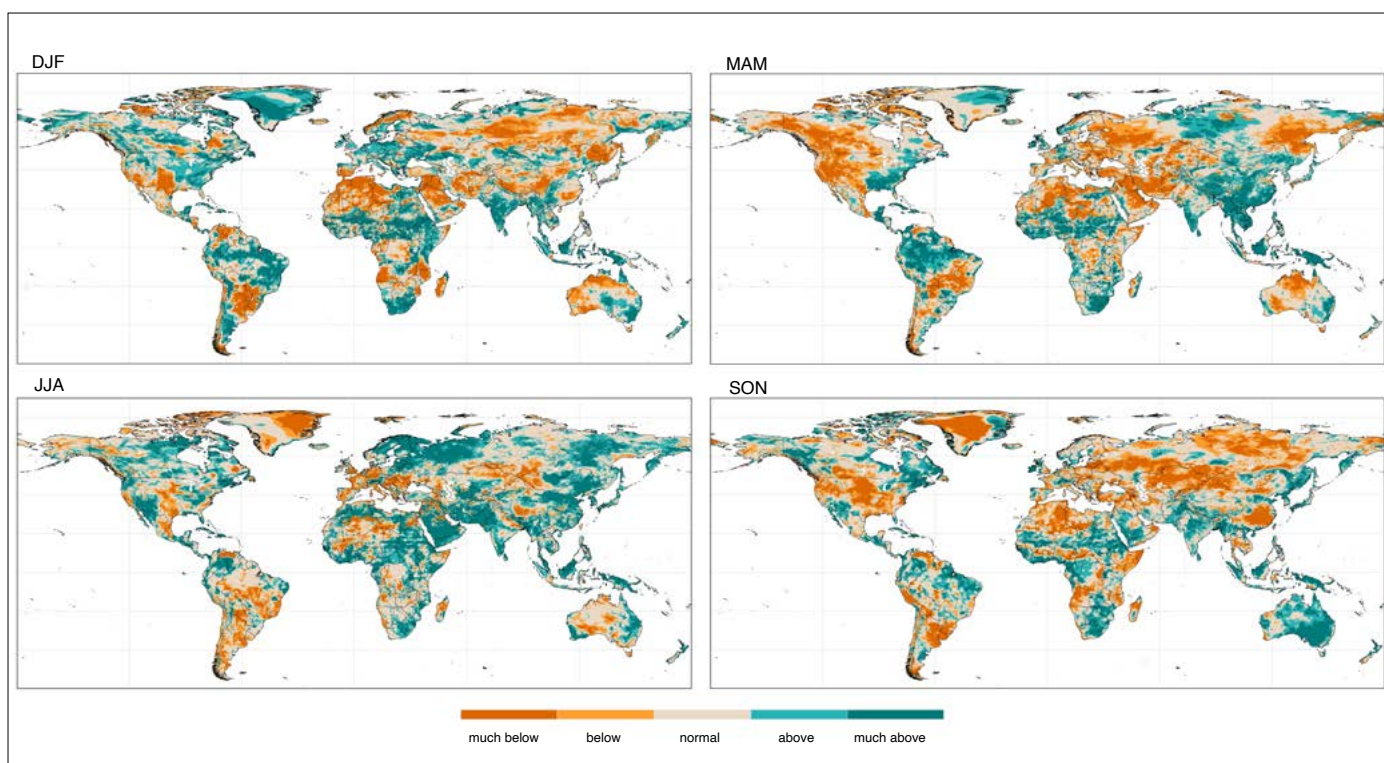


Figure 8. Seasonal anomaly in evapotranspiration (ET) in 2022 as ranked with respect to the historical period 2003–2020.

Note: DJF – December–January–February (includes December 2021), JJA – June–July–August, MAM – March–April–May, SON – September–October–November.



On the west coast and in the central part of the United States, due to limited water availability associated with drought conditions, ET was lower than normal over the March–April–May (MAM) and September–October–November (SON) periods of 2022. Parts of the Mackenzie and Yukon basins in Northern North America also exhibited below-normal to much-below-normal trends in ET over the spring period.

Australia presented a contrasting picture during the year 2022. The south-eastern part of the country, particularly in the Murray–Darling river basin, exhibited higher ET throughout the year, with this trend being most pronounced in SON. In contrast, parts of west and north-west Australia showed decreased ET over the December–January–February (DJF) and MAM periods.

A similar pattern of varying ET over the year 2022 was observed in Middle Eastern countries, particularly western Islamic Republic of Iran, Syrian Arab Republic and Iraq. These areas saw below-normal ET during DJF and MAM but experienced above-normal ET during June–July–August (JJA).

In Pakistan and India, ET was much above normal during the monsoon period, due to increased temperatures and above-normal water availability. This period was characterized by extreme rainfall and associated significant flooding.⁷⁶ This situation persisted through SON when the territory of Pakistan was still partially flooded.

The La Plata river basin and the Horn of Africa were identified as below-normal hotspots due to the continued drought, which limited the available water for ET. Also, China’s Yangtze river basin experienced significantly-below-normal ET in SON, subsequent to the heatwave, due to a scarcity of available water.

The ET across Europe in DJF was above normal, except for Southern Europe, in particular southern Italy, Spain and Portugal. Over MAM, JJA and SON a gradual drop in ET occurred, with ET hitting the lowest values during JJA in Spain, Portugal, Italy, France and Germany. This could be attributed to the summer heatwave and drought-related reduced water availability.

Terrestrial water storage

Satellite gravimetry is a remote-sensing-based method (used in GRACE and GRACE-FO)^{77,78} capable of observing all mass changes, in particular those caused by water storage changes, including in surface water, soil moisture, groundwater, as well as snow and ice. Terrestrial water storage (TWS) is expressed as an anomaly relative to its long-term mean in equivalent water heights in centimeters as an area-averaged height of the water column over the area being considered. The section on [TWS](#) in Annex 1 provides more details on TWS and how TWS anomalies were calculated.

Figure 9 provides the TWS anomalies for 2022 in comparison to the 2002–2020 historical period, and Figure 10 presents long-term trends in TWS around the globe over the 2002–2022 period. The TWS observations for 2022 reflect the anomalies presented in the previous chapters for other variables and further emphasize several critical hotspots for the year 2022.

In particular, the headwaters of the La Plata river basin, the south-western United States, North Africa, the entire Middle East region, Central Asia and large parts of Europe showed below-normal and much-below-normal TWS. These areas were characterized by limited water availability in 2022, which is mirrored in their decreased TWS. For most parts of Europe, for instance, the TWS trends (Figure 10) over the observation period of satellite gravimetry from 2002 to 2022 exhibit slightly negative values (that is, an overall decrease in TWS). However, these negative trend values are hardly visible in Figure 10, as the plot is dominated by much larger negative trends in other regions of the world, related to the melt of glaciers and ice caps, or groundwater depletion, for instance.

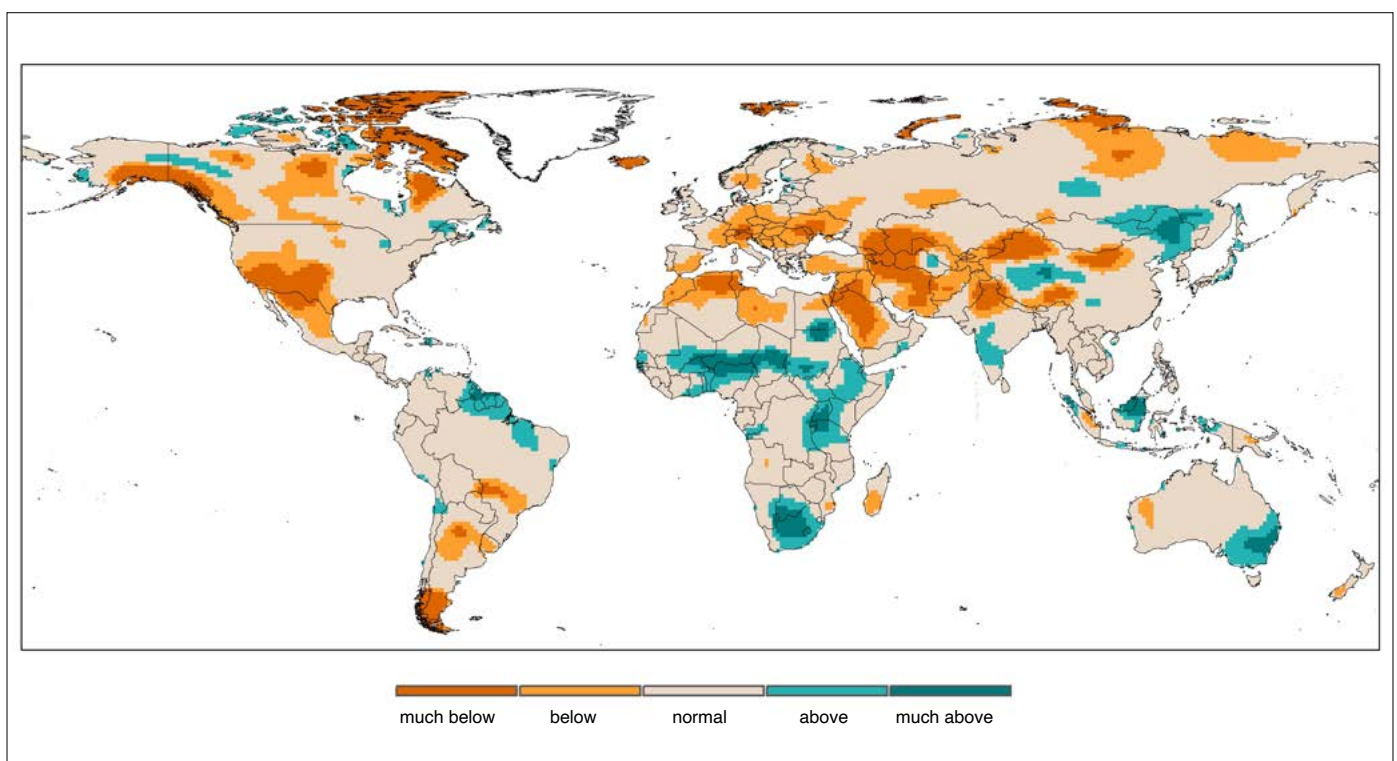


Figure 9. Terrestrial water storage anomalies in the year 2022 ranked with respect to the historical period 2002–2020, that is, the same reference period as for the *State of Global Water Resources 2021* (WMO-No. 1308). Note that Greenland and Antarctica are not included, as their mass balance trends are large and therefore overshadow the other continental mass balance trends depicted here.

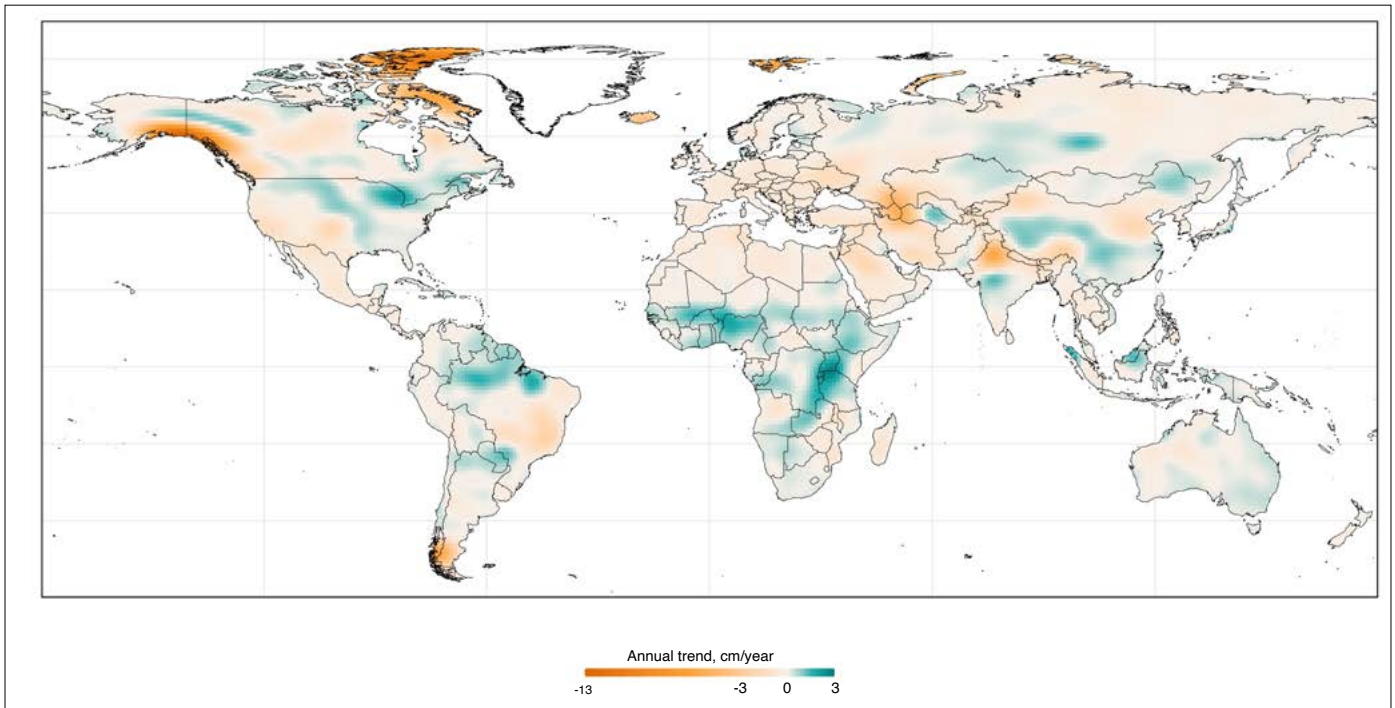


Figure 10. Trends in terrestrial water storage over the period 2002–2022. Note that Greenland and Antarctica are not included, as their mass balance trends are large and therefore overshadow the other continental mass balance trends depicted here.

The flood event in Pakistan did not lead to an increase in TWS in the annual anomaly, because until June 2022 dry TWS conditions prevailed in the region due to an extreme heatwave before the flooding that also led to significant snow and ice melt in the upper part of the Indus basin. The strong increase in TWS in the second half of 2022 during the flood event is averaged out in the annual TWS anomaly values used for Figure 10. The Sahel region and, partially, the Murray–Darling basin in Australia, which exhibited above-normal discharge conditions and were affected by floods, also show above-normal and much-above-normal TWS in 2022 (Figure 9). Also, large parts of southern Africa stand out with above-normal TWS conditions, in line with above-normal conditions of reservoir inflow shown above. Overall, there is a positive TWS trend in the Sahel region and large parts of eastern and southern Africa from 2002 to 2022 (Figure 10).

The Horn of Africa, despite enduring a persistent drought, is not characterized by below-normal TWS on average for the year 2022. The reason is that the region and large parts of East Africa experienced a marked TWS increase in the years 2019–2020 that led to clearly above-normal TWS anomalies. The effects of this period are still seen in the TWS data of 2022, where the recent drought led to a return to the normal TWS range but not yet to below-normal conditions.

Year 2021 and 2022 anomalies in TWS show similar patterns, revealing several hotspots with strong negative TWS anomalies, for example in North Africa, parts of the Ganges and Indus headwaters, parts of the Middle East as well as the south-western United States. The Niger basin, East African Rift and northern Amazon basin showed positive anomalies.

Snow cover and glaciers

This section consists of contributions by WMO Member States and Territories and WMO experts (see acknowledgements for further details) and provides examples of changes in the snow patterns and glaciers in several regions of the world in the recent period, with a focus on the 2022–2023 snow year.

CENTRAL EUROPE AND THE ALPS

The snow cover area in the Alps remained well below the 30-year average during the 2023 spring despite late snowfalls in May (Figure 11), as observed in the basins feeding the four major rivers, Rhine, Rhône, Danube and Po (Figure 12). The same pattern can be observed in every major alpine catchment, but the situation was more severe in the Po river basin.

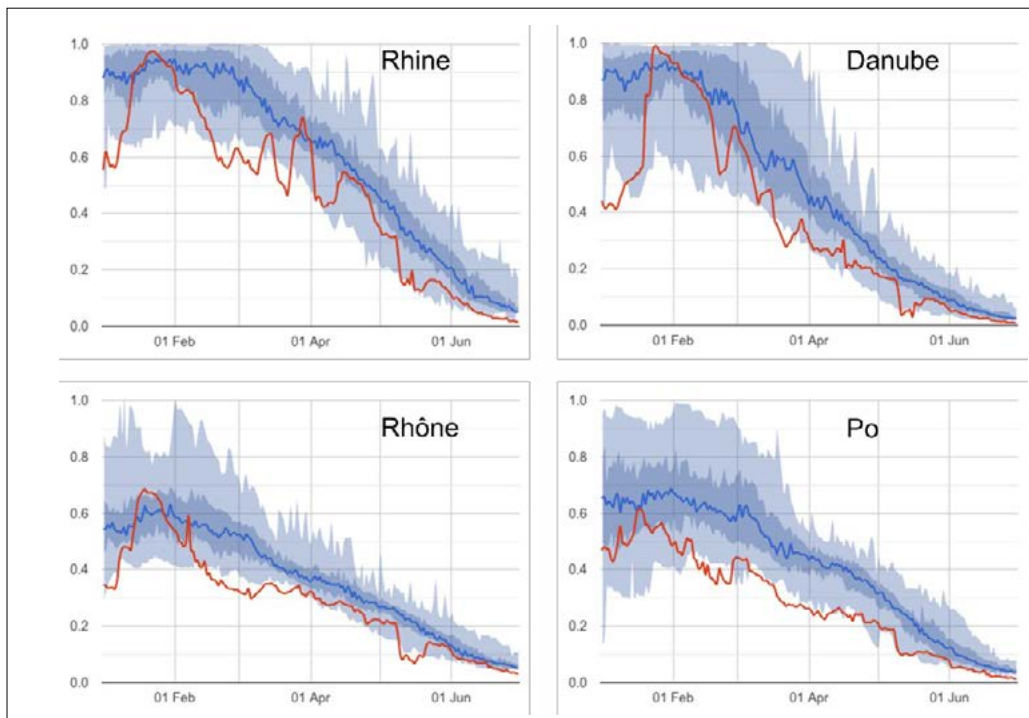


Figure 11. Snow cover fraction for the Rhine, Rhône, Danube and Po catchments. The blue line shows the median daily snow cover from the 30-year average, with the shaded zones representing the four quartiles, and the red line represents the 2023 assessment. *Source:* Gascoin, S., Monteiro, D., Morin, S. Reanalysis-based Contextualization of Real-time Snow Cover Monitoring from Space. *Environmental Research Letters* **2022**, 17(11), 114044. <https://doi.org/10.1088/1748-9326/ac9e6a>.

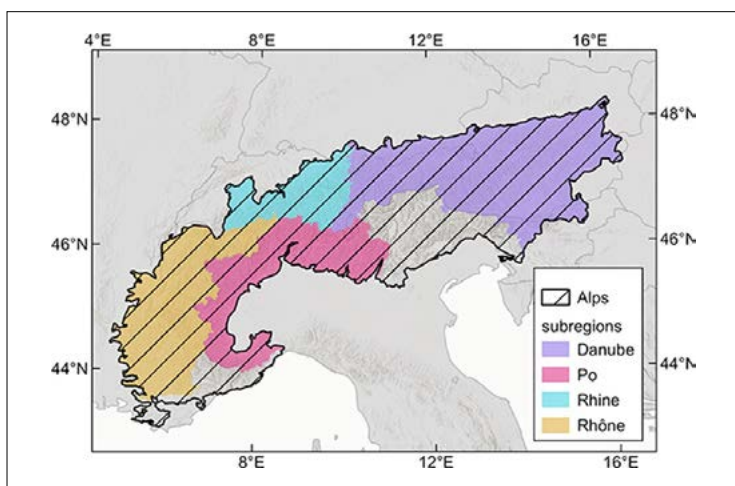


Figure 12. Outlines of major Alpine river basins. *Source:* Gascoin, S., Monteiro, D., Morin, S. Reanalysis-based Contextualization of Real-time Snow Cover Monitoring from Space. *Environmental Research Letters* **2022**, 17(11), 114044. <https://doi.org/10.1088/1748-9326/ac9e6a>.

SUBTROPICAL ANDES

The winter snow in the subtropical Andes regulates the flows of mountain rivers across central Chile and central-western Argentina and provides the largest volumes of water for recharging the aquifers used on both sides of the Andes, for cities like Santiago (Chile) and Mendoza (Argentina).

Since 2009–2010, the region’s winter snow accumulation has declined substantially, resulting in an extended period of drought locally known as “mega-drought”. Analyses of the snow-covered areas indicate that the winter of 2021 showed the lowest snow accumulation values on record, while during the winter of 2022, the snow amounts reached slightly above-average conditions in some areas (Figure 13), with below-average conditions persisting along the central watersheds between $\sim 32^\circ$ and $\sim 37^\circ$ S, especially along the eastern side of the Andes (Argentina). As these watersheds contain the most heavily populated urban centres of the region, water shortages have continued, and the local governments have kept water restriction measures in place.

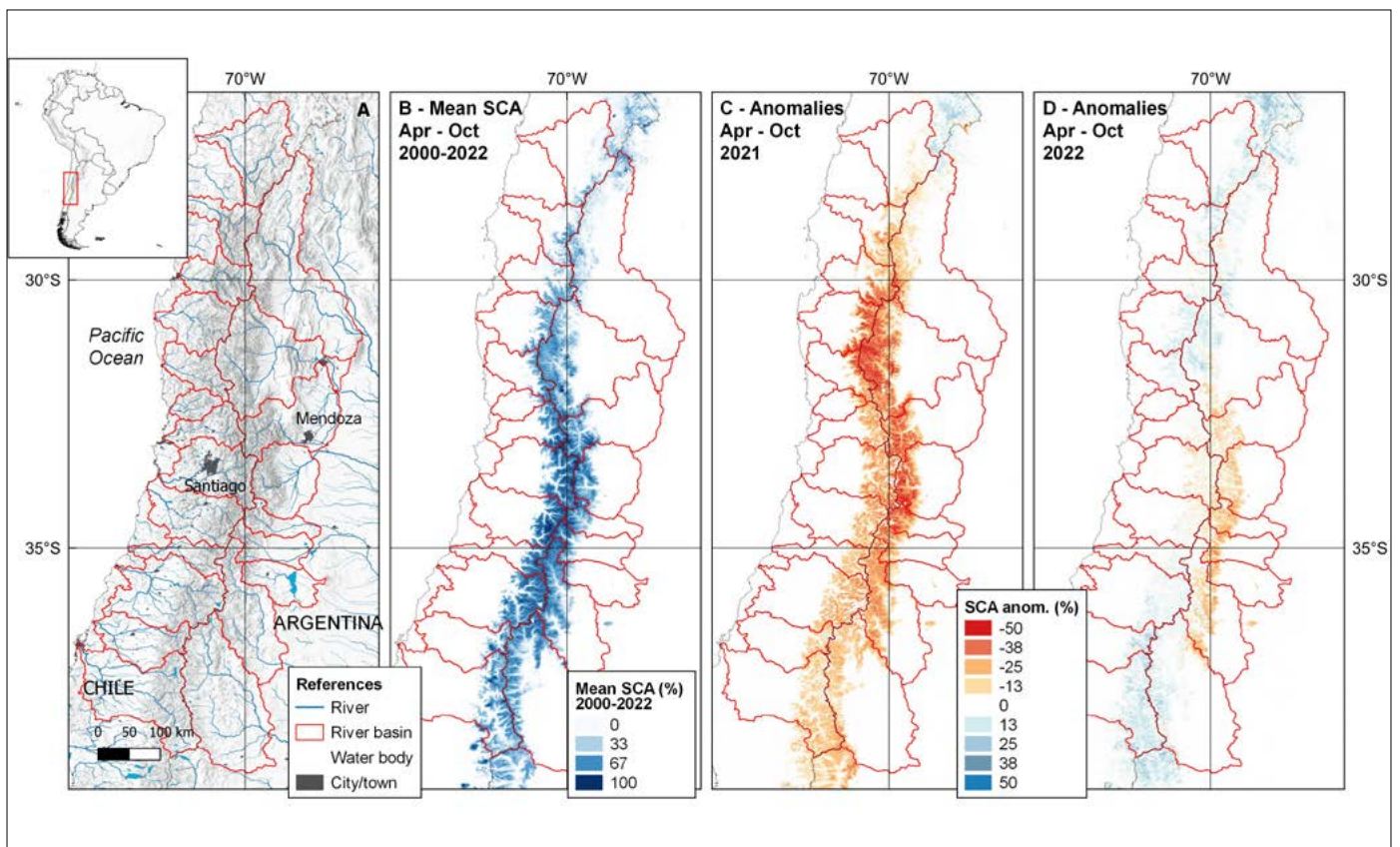


Figure 13. (a) Map of the Andes in Chile and Argentina between $\sim 27^\circ$ and $\sim 39^\circ$ S (the shading indicates topography). (b) Mean cold-season (April–October) snow-covered area (SCA). (c) Cold-season SCA anomalies for 2021. (d) Cold-season SCA anomalies for 2022.

Source: [Observatorio de Nieve en los Andes de Argentina y Chile](#).

CRYOSPHERE CHANGES AND WATER RESOURCES MANAGEMENT IN CENTRAL ASIA

Over the last decade increasing attention has been paid to monitoring of the Central Asian cryosphere due to its critical role in regional water security and vulnerability to global climate change (Figures 14 and 15). Several projects supported by the international community have focused on glacier monitoring, high-altitude hydrometeorological observations, permafrost and seasonal snow cover, aimed at building and sustaining regional and national capacity for and enabling long-term understanding of cryospheric changes and monitoring impacts on water resources and other environmental changes.⁷⁹

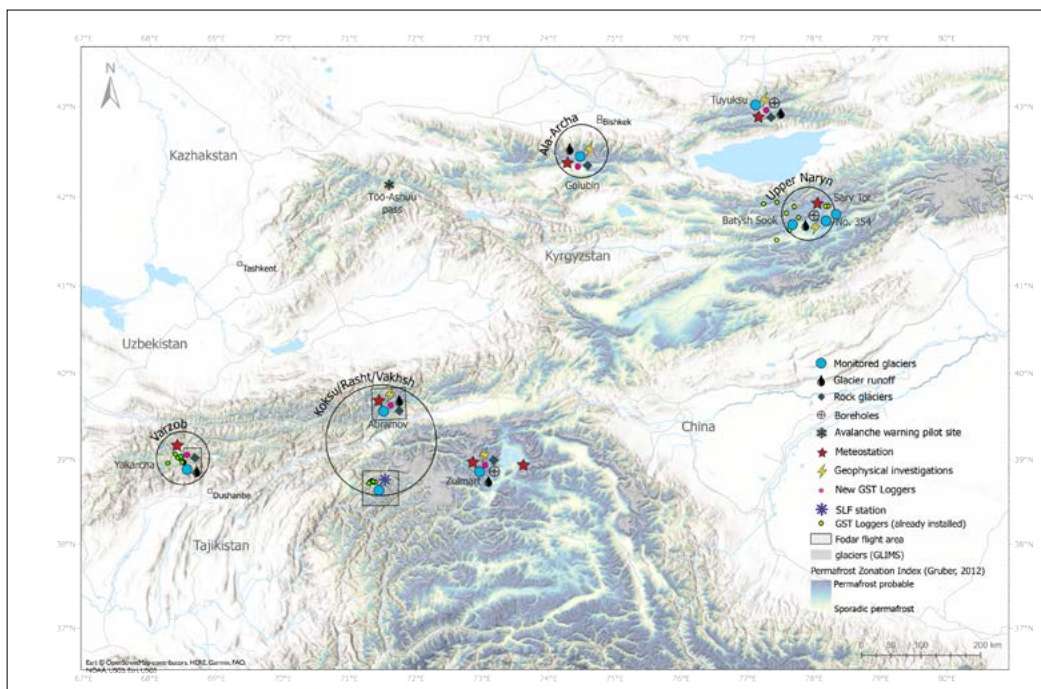


Figure 14. Cryosphere monitoring network in Central Asia (with contributions from the CATCOS, CICADA and CROMO-ADAPT projects supported by the Swiss Agency for Development and Cooperation).

Source: University of Fribourg/CROMO-ADAPT.

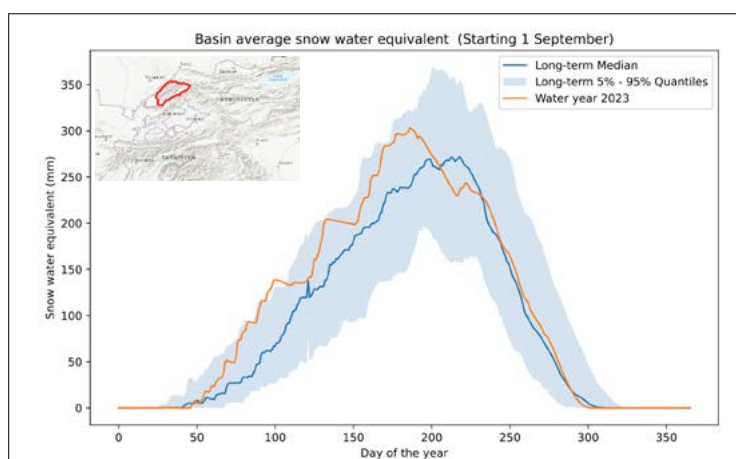


Figure 15. An example of a snow tracker using a mixture of models and remote sensing data to give real-time analysis of snow water equivalent anomalies at basin scale (the standard water year covers 1 September to 30 August the following year; this figure shows the 2022/2023 standard water year).

Credit: WSL Institute for Snow and Avalanche Research SLF/CROMO-ADAPT.



STATUS OF GEORGIAN GLACIERS

In Georgia, on the ridge of the Greater Caucasus, there are well-developed, high-elevation glaciers (as high as 5 174 m).

Since the 1960s, climate change has led to the disappearance of 29% of Georgia’s glaciers, and the area covered by glaciers has decreased by 30.3%. This has had direct impacts on the water balance and on downstream water users, as well as being linked to degradation of landscapes, contribution to the increase in the level of the Black Sea, and growth in the frequency and intensity of natural disasters of glacial origin, with material and human losses.

The retreat of the Shkhara glacier provides a good illustration of the accelerated melting of the Georgian glaciers over the last half-century. Data from LANDSAT and from field observations by the Department of Hydrometeorology of Georgia show that the speed of retreat of the Shkhara glacier has increased from approximately 6.5 m/year to approximately 14.7 m/year (Figure 16). A similar change was observed for other large glaciers in Georgia.

ASIAN WATER TOWER

The Third Pole, encompassing the Tibetan Plateau, the Himalayas, the Karakorum, the Hindu Kush, the Pamirs and the Tien Shan Mountains, is characterized as the Asian Water Tower (AWT), and is the most important and most vulnerable among the water towers of the world. The AWT is the planet’s largest reservoir of ice and snow after the Arctic and Antarctic regions. It provides a reliable water supply to almost 2 billion people.

Glacial melting is accelerating in the region. From 2000 to 2018, total glacier mass in the AWT decreased by approximately 4.3%, in a heterogeneous spatial pattern with the greatest magnitude of melting in the south-eastern Tibetan Plateau and smaller retreat or even gain in mass in the Karakoram, western Kunlun and eastern Pamirs. Permafrost degradation is evident, characterized by thickening of the active layer, rising of ground temperature and

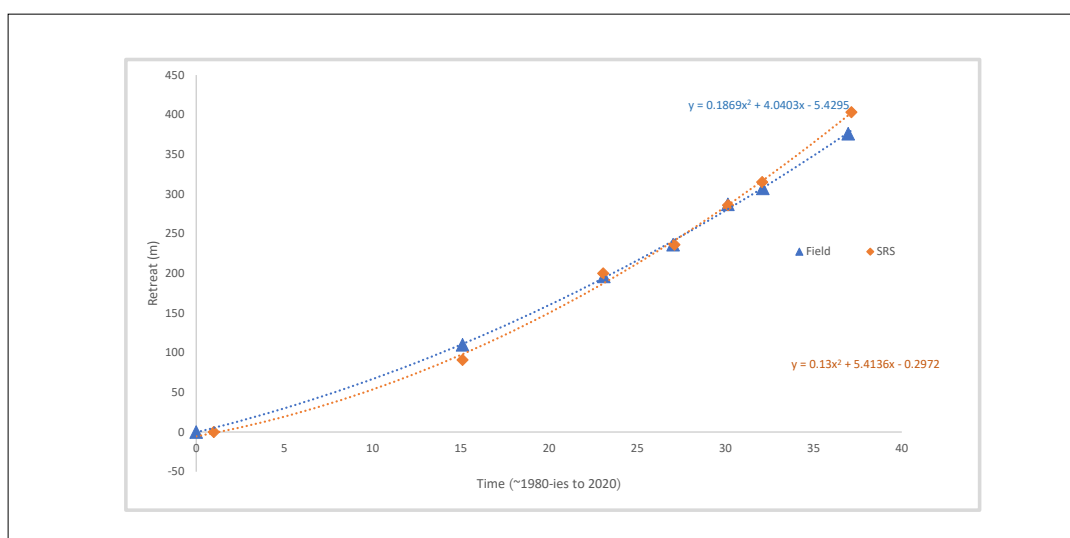


Figure 16. Graph of the retreat of the Shkhara glacier. The blue curve is based on ground observations, and the orange curve is based on satellite remote sensing (SRS) data.

shortening of frozen duration of active layer. Snow cover area has significantly decreased, and the snowmelt season has shortened. The number, total area and volume of glacier lakes have increased rapidly as a whole, and the total water mass in lakes has increased by approximately 16% of the total lake volume.

During 1980–2018, annual river run-off across most of the AWT showed a significant increase in rivers such as the upper Indus (+3.9 gigatons (Gt) of river run-off, including glacier melt mass, precipitation and snow melt induced run-off, per decade) but was stable in rivers such as the Yangtze and Salween, while a decline in run-off was observed in the Yellow River (−1.5 Gt river run-off per decade).

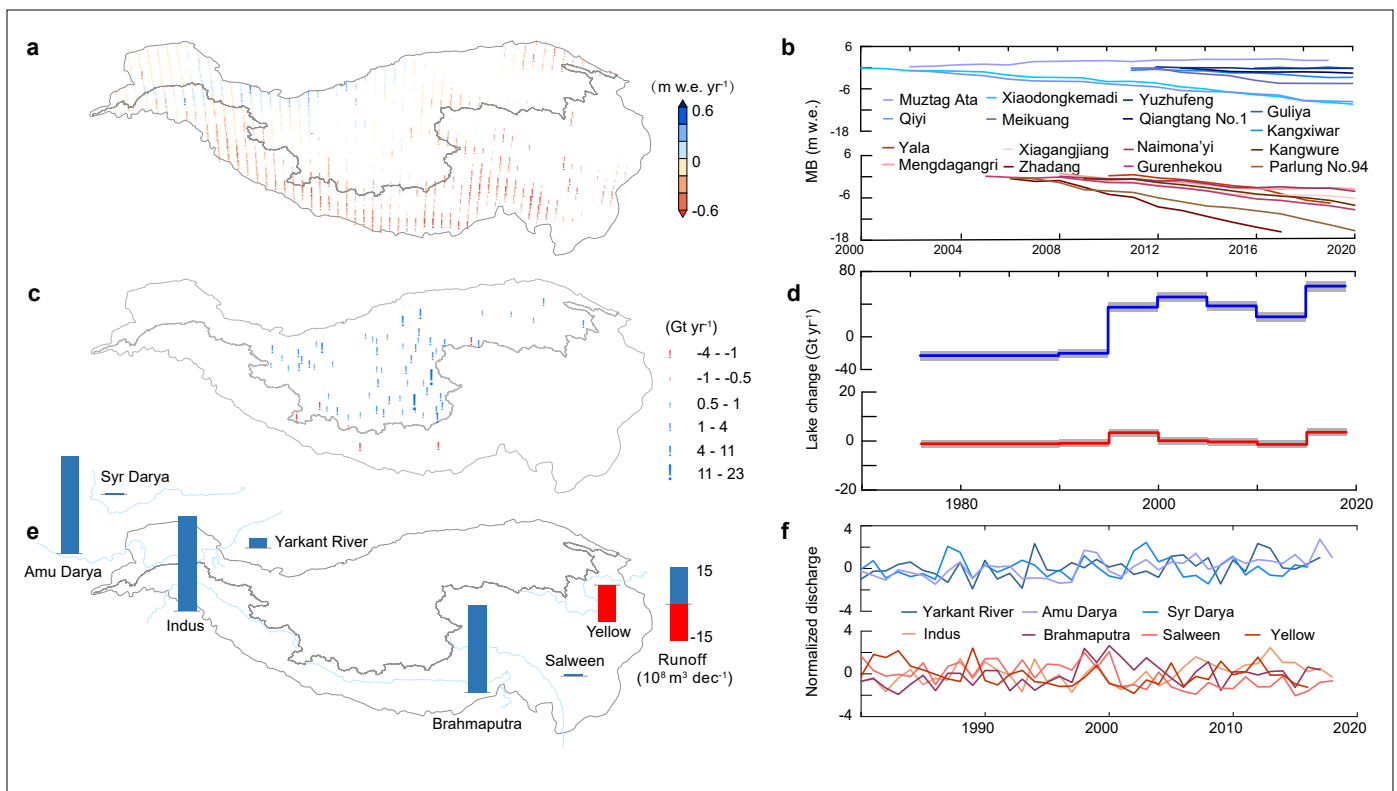


Figure 17. Observed changes in glaciers, lakes and run-off over the AWT. (a) Spatial patterns in glacier mass balance between 2000 and 2018 based on digital elevation models. (b) Eight continuous mass balance measurements in endorheic basins and eight in exorheic basins. (c) Spatial pattern of basin-wide lake volume changes between 1976 and 2019. (d) Time series of total lake volume changes in endorheic and exorheic basins. (e) Spatial pattern of run-off trends for seven large rivers. (f) Time series of run-off for three rivers in endorheic basins and four rivers in exorheic basins. The Yarkant River, Amu Darya and Syr Darya are endorheic rivers, while the Indus, Brahmaputra, Salween and Yellow are exorheic rivers.

SNOW WATER EQUIVALENT IN CANADA

In many parts of Canada, March snow water equivalent (SWE) provides a proxy for seasonally maximum SWE and can be estimated from a combination of assimilated in situ data, satellite passive microwave retrievals and historically forced snow models using the approach reported by Mudryk et al.⁸⁰ March 2022 SWE anomalies are presented as percent differences with respect to the 1991–2020 average (Figure 18). Large portions of south-central and south-eastern Canada had above average SWE in March 2022, though there were particular areas of the southern Rocky Mountain and prairie region along the Canada–United States border with well-below-average SWE conditions. Areas of north-central Canada, including parts of the Northwest Territories, had below-average SWE in March 2022, while areas north of the Arctic Circle had SWE varying from slightly below to slightly above the 1991–2020 average.

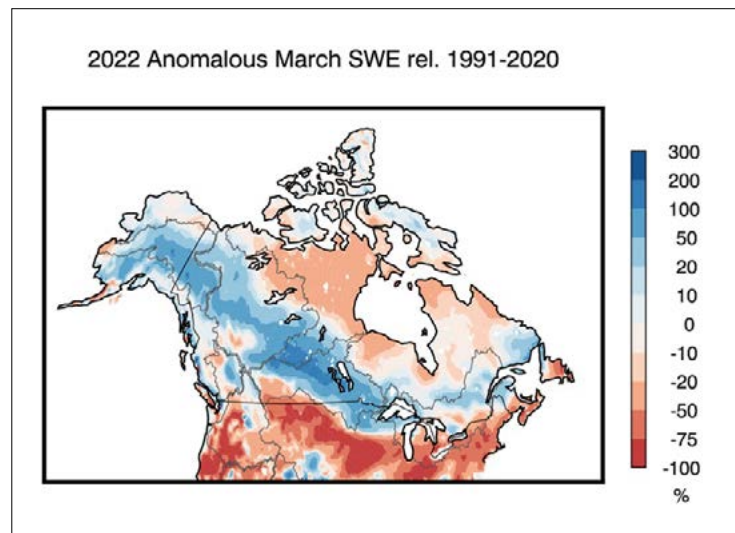


Figure 18. Anomalous March snow water equivalent for 2022 with respect to 1991–2020 average values

High-impact hydrological events

This chapter presents a non-exhaustive review of selected major extreme events that occurred in 2022. The events were selected based on the number of casualties (>100) or overall impact on people affected/displaced, using data from several sources, including the EM-DAT database,⁸¹ the WMO *State of the Global Climate 2022* (WMO-No. 1316) and other public sources such as the World Bank⁸² and ReliefWeb (Figure 19).

PAKISTAN, INDIA AND BANGLADESH FLOODS

Over 33 million people were affected by flooding in Pakistan, which took place during an exceptionally rainy monsoon period in 2022. July 2022 saw 181% of normal precipitation, and in August 243% of normal precipitation fell.⁸³ This excessive rainfall, combined with glacial lake outburst floods,^{84,85} led to severe flooding, with 94 districts inundated⁸⁶ (about 9% of Pakistan's total area). There were more than 1 700 deaths,^{87,88,89} and economic losses of up to US\$ 30 billion.^{90,91} Due to the flat orography and low drainage capacity, some affected areas remained inundated for several weeks.

India and Bangladesh were also affected by floods in 2022. In India, about 700 people died during the monsoon season (particularly in the north-east of the country, in June) from flooding and landslides,^{92,93} and in Bangladesh, flooding affected 7 million people and caused 141 deaths.⁹⁴

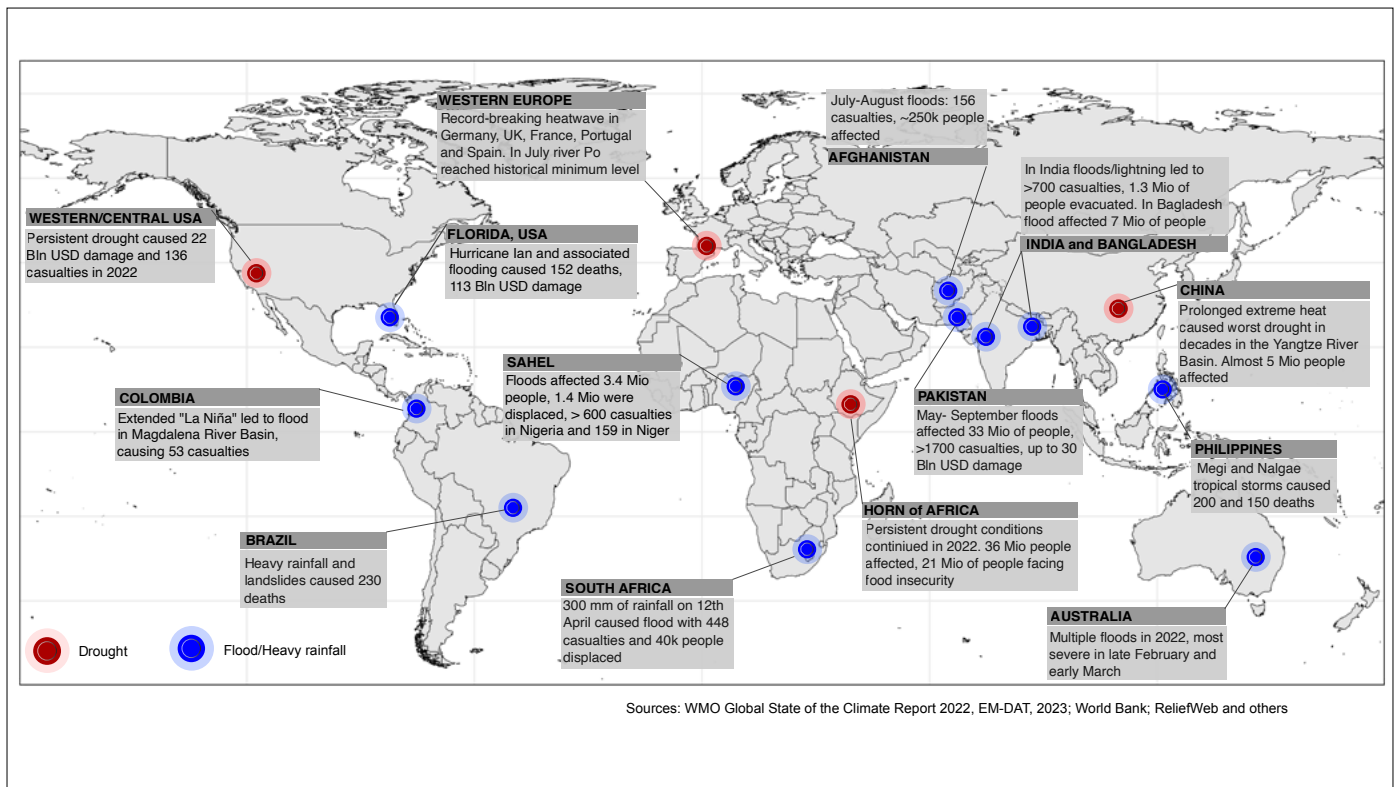


Figure 19. Selected notable high-impact hydrological events across the globe in 2022; circles indicate flood (blue) and drought (red) events



SAHEL FLOODS

Heavy precipitation towards the end of the monsoon period (October–December) caused flooding in Nigeria, Niger, Chad and southern Sudan. In Nigeria, the situation was exacerbated by excessive rainfall in October. In total more than 600 people lost their lives to flooding in Nigeria and 159 in Niger.^{95,96} In Niger, the associated economic losses reached US\$ 4.2 billion.⁹⁷

DROUGHT IN THE HORN OF AFRICA AND CENTRAL AFRICA

2022 was the third consecutive year with low rainfall in the Horn of Africa.⁹⁸ Across the Horn of Africa, at least 36.1 million people were affected by severe drought in October 2022.⁹⁹ About 4.9 million children were acutely malnourished in drought-affected areas, of whom about 2.2 million were in Ethiopia, 884 500 in Kenya and 1.8 million in Somalia.¹⁰⁰ In addition, up to 24 million people were confronting dire water shortages by December 2022.¹⁰¹

EXTREME AND LONG-TERM DROUGHT IN LA PLATA BASIN

Drought conditions in the La Plata basin in Brazil–Argentina in 2022 were the most severe since 1944, impacting agriculture by reducing crop production and affecting global crop markets.¹⁰² The drought conditions caused a significant drop in hydropower production in 2022, resulting from low river flows.¹⁰³

SUMMER HEATWAVE IN EUROPE

Many rivers in Europe were affected by the extreme heatwave and drought conditions during the summer of 2022 – for example, the Rhine, Loire, Danube and Po Rivers fell to critically low levels.¹⁰⁴ Impacts were felt across Europe on water resources, agriculture and the environment. In Italy, the Po River experienced the worst hydrological drought in 216 years, with a return period of six centuries.¹⁰⁵ The drought threatened crop production in the Po Valley, where 40% of crops in the country used to be produced,¹⁰⁶ often under irrigated conditions.

In France, the low river flows and elevated river-water temperatures led to a reduction in the output of nuclear power stations due to the lack of cooling water.¹⁰⁷

During the July–August 2022 heatwave in the UK, soil moisture levels reached exceptionally low values, resulting in impermeable and arid landscapes. This phenomenon contributed to a threefold increase in wildfires and significant challenges for agriculture. Record-low water levels were observed in reservoir stocks, along with record-low river flows comparable to the historic drought of 1976.^{108,109}

In 2022, the European Alps witnessed unprecedented levels of glacier mass loss. The reduction was significantly beyond historical fluctuations. In just a year, from 2021 to 2022, Switzerland experienced a 6.2% decline in its glacier ice volume.¹¹⁰

Synthesis

The 2022 edition of the State of Global Water Resources report has introduced several important advancements. First, the representation of the state of global water resources provided by the report was enhanced through the incorporation of new chapters portraying additional components of the hydrological cycle: groundwater, soil moisture, evapotranspiration, reservoir inflows, and snow and ice. Data for these additional components were received through the integration of observation, satellite-based remote sensing data and outputs from numerical modelling simulations.

Second, there was a substantial increase in the amount of observed discharge data available for analysis for 2022: discharge data were received from nearly 500 stations, which after quality control was reduced to 273 stations, as compared to the 38 stations utilized in the report from the previous year. However, data from only 14 countries were available for this report, leaving regions such as Africa, the Middle East and Asia notably underrepresented in terms of available observational data.

Third, the spatial resolution of global analysis has been refined, reaching a total of 986 river basins globally. Also, the number of the GHMSs contributing to the 2022 edition of the report increased, which has contributed to the robustness of the discharge estimates. At the same time, in some areas (such as the United Kingdom) the basin resolution was still not optimal and will need to be refined in the future editions of the report. The agreement of the GHMSs on the sign of changes is presented in [Figure A3](#) and [Figure A4](#) of Annex 1.¹¹¹

Increased availability of observed data, and contributions from the Member States and Territories for validation of the modelled results have allowed for a more accurate and reliable portrayal of the hydrological cycle, on both a global and regional/local scale. For future annual editions of the report, the objective remains to steadily enhance and augment the accessibility of observational data.

In 2022, over 50% of global catchment areas experienced deviations from normal river discharge conditions. Most of these areas were drier than normal, while a smaller percentage of basins displayed above-normal or much-above-normal conditions. When compared to 2021, the scenario was somewhat similar, however, in 2021 a greater number of rivers experienced dry to normal conditions (Figure 20). Water inflow into a selection of major reservoirs considered in this report in 2022 followed the trend in general discharge – more than 60% of reservoirs saw below-normal or above-normal inflow.

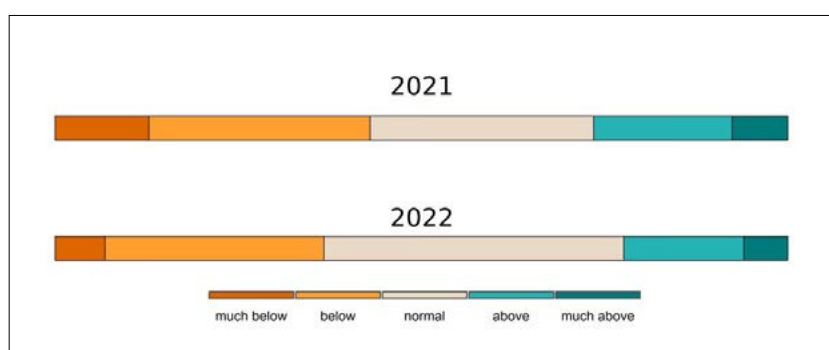


Figure 20. The distribution of the area under different river discharge conditions for the years 2021 and 2022. The results for the year 2021 were recalculated according to the method used for the year 2022 (Box 1).



Throughout 2022, soil moisture and evapotranspiration, as well as TWS anomalies echoed the anomalies in discharge conditions and significant extreme events of the year. Several regions around the world continued to endure severe droughts, notably the United States, the Horn of Africa and the La Plata basin. In addition, severe droughts hit large parts of North Africa, Europe, the Middle East and China. Europe, in particular, suffered an extreme heatwave and a record-breaking drought, leading to critically-low levels in several rivers such as the Po, Danube, Rhine and Loire, and severely affecting navigation in the Danube and Rhine. In France, increased temperatures coupled with low water levels resulted in a decrease in electricity production from nuclear plants due to insufficient cooling water. Also, navigation on the Mississippi River was affected by the extremely low water levels, as a result of a continuing drought in the United States. These areas also saw depleted inflows into reservoirs, and decreased soil moisture and evapotranspiration levels. In South America, the La Plata river basin has endured a continuation of drought conditions since 2020, as evidenced by reduced discharge and decreased soil moisture and evapotranspiration.

The year 2022 brought a mix of extreme weather conditions to Asia and Oceania. Severe drought in the Yangtze river basin in China led to much-lower-than-average river discharge, inflow to reservoirs and soil moisture. In contrast, a mega-flood hit the Indus river basin in Pakistan during the monsoon period, leading to about 9% of the country's territory being inundated and huge losses in terms of casualties and the economy. In fact, part of the country remained inundated for several weeks after the major event was over. Reservoirs in India and Pakistan saw above-average inflow due to high discharge conditions and flood events. In eastern Australia, the Murray–Darling River basin experienced several flood events throughout 2022.

Africa witnessed contrasting situations. The Horn of Africa continued to suffer from a long-lasting severe drought threatening the food security of 21 million people, with much-below-average water availability levels. Yet, the Niger basin and much of South Africa recorded above-average discharge, linked to major flood events in 2022.

In 2022, the snow cover in the Alps, crucial for feeding major rivers like the Rhine, Danube, Rhone, and Po, remained significantly below the 30-year average despite late snowfalls in May. Additionally, in 2022, the European Alps witnessed unprecedented levels of glacier mass loss. The reduction was significantly beyond historical fluctuations. Increasing melting of glaciers, and changing patterns of rainfall and snowfall, associated with climatic change, may lead to a change of the discharge regime to a more pluvial one in the Rhine river basin.¹¹² Meanwhile, the subtropical Andes have been experiencing a consistent decline in winter snow accumulation since 2009, impacting water supplies for cities across Chile and the west of Argentina. Although 2022 saw slightly-above-average snow in some areas, key watersheds still reported below-average conditions, especially on the Argentinean side, leading to sustained water restrictions in populous urban centers. Georgia's glaciers have undergone alarming shrinkage, with the retreat of the Shkhara glacier being a key example, with a melting rate that nearly doubled in recent years. The Third Pole, encompassing the Tibetan Plateau, the Himalayas, the Karakorum, the Hindu Kush, the Pamirs and the Tien Shan Mountains, vital for almost 2 billion people's water supply, observed pronounced glacial melting between 2000 and 2018, with permafrost degradation becoming more pronounced, decrease in snow cover, shortening of the snowmelt season and increase in the number, total area and volume of glacier lakes. This critical water source caused significant variability in river run-offs in the Indus, Amu Darya, Yangtze and Yellow river basins, indicating climate change's evolving influence on the region.

Some global circulation patterns, such as La Niña or the Indian Monsoon, provide clear evidence of their impact through the hydrological variables, namely soil moisture and run-off. However, it is obvious that understanding the hydrological cycle at the sub-continental scale

(basin scale) is critical for understanding it at the global level, as maps of categorization of flow demonstrate quite scattered patterns on all continents. At the same time, the importance of initial hydrological conditions (for example, snow accumulation and soil moisture) is obvious in some areas, as they carry the deviation or signal over seasons. This supports the importance of initial hydrological conditions as the most important predictor for sub-seasonal to seasonal hydrological forecast for certain regions and seasons.¹¹³

Box 4

NEXT STEPS: WMO'S HYDROSOS TO FEED INTO THE FUTURE STATE OF GLOBAL WATER RESOURCES REPORTS

The goal is for future versions of this report and others like it is to base such reporting on increased ground data availability. Increased contribution from and participation by WMO Members and other partners will support larger coverage of in situ data. This will be supported by the WMO Hydrological Status and Outlook System (HydroSOS), which is currently under implementation at various spatial scales (Figure 21). HydroSOS provides assessment and reporting on the current status of the water resources in a basin and whether the status is likely to change in the future on a sub-seasonal to seasonal scale. HydroSOS builds on the existing system and capacities of the relevant national and regional hydrological authorities.

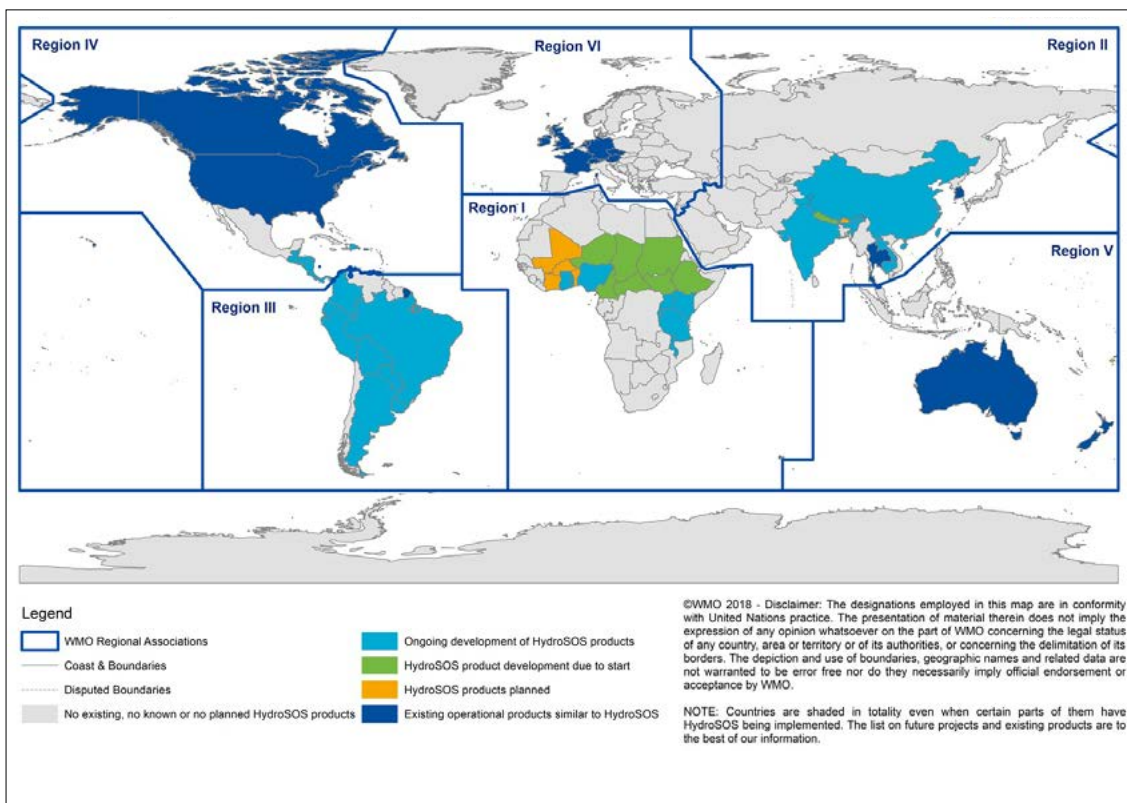


Figure 21. Status of HydroSOS implementation at various scales around the globe (updated in July 2023)



Annual TWS anomalies provide complementary information in addition to observations and modelled data on discharge, ET and other types of water storage (for example, soil moisture, reservoirs and snow and ice) to more completely understand the variations in the hydrological cycle over a given year. Also, the need for accounting for a typical hydrological regime (that is, seasonal variations in hydrological variables) in a given basin is critical for correct interpretation of the status of water availability and its potential impacts on human society and ecosystems.

Data on more components of the hydrological cycle have helped this report to more fully portray the state of water resources globally as well as locally, and enhanced understanding of hydrological events that occurred in 2022. Increasing the availability of observed data is crucial to accurately understand the real-world mechanisms of the hydrological cycle and improve the output of assessment reports, including those related to groundwater.

Endnotes

- ¹ In this report, the term anomaly refers to presentation of the status of water resources in each basin in comparison to the long-term historical near-normal conditions for that basin.
- ² Historical periods differ from variable to variable; refer to Table 1 of Annex 1.
- ³ Note that throughout the text the term “normal” refers to near-normal conditions for each variable.
- ⁴ For information on the reference period used for each variable, refer to Table 1 of Annex 1. Note that selection of different reference periods may influence the calculated trends.
- ⁵ Global Runoff Data Centre (GRDC). *WMO Basins and Sub-Basins*; 3rd rev. ext. ed., Federal Institute of Hydrology (BfG): Koblenz, Germany, 2020.
- ⁶ Data courtesy of the Global Runoff Data Centre, Koblenz, Germany.
- ⁷ van Verseveld, W. J.; Weerts, A. H.; Visser, M. et al. Wflow_sbm v0.6.1, a Spatially Distributed Hydrologic Model: From Global Data to Local Applications. *Geoscientific Model Development Discussions* **2022**, 1–52. <https://doi.org/10.5194/gmd-2022-182>.
- ⁸ Yamazaki, D.; Kanae, S.; Kim, H. et al. A Physically Based Description of Floodplain Inundation Dynamics in a Global River Routing Model. *Water Resources Research* **2011**, 47(4). <https://doi.org/10.1029/2010WR009726>.
- ⁹ Arheimer, B.; Pimentel, R.; Isberg, K. et al. Global Catchment Modelling Using World-Wide HYPE (WWH), Open Data, and Stepwise Parameter Estimation. *Hydrology and Earth System Sciences* **2020**, 24(2), 535–559. <https://doi.org/10.5194/hess-24-535-2020>.
- ¹⁰ Kumar, S. V.; Mocko, D. M.; Wang, S. et al. Assimilation of Remotely Sensed Leaf Area Index into the Noah-MP Land Surface Model: Impacts on Water and Carbon Fluxes and States over the Continental United States. *Journal of Hydrometeorology* **2019**, 20(7), 1359–1377. <https://doi.org/10.1175/JHM-D-18-0237.1>.
- ¹¹ Nie, W.; Kumar, S. V.; Getirana, A. et al. Nonstationarity in the Global Terrestrial Water Cycle and its Interlinkages in the Anthropocene. *Research Square* **2023** [preprint].
- ¹² *A Global Reanalysis for Water, Energy, and Carbon Cycle Variables Overview*. <https://www.earthdata.nasa.gov/dashboard/data-catalog/global-reanalysis-da>.
- ¹³ Landerer, F. W.; Flechtner, F. M.; Save, H. et al. Extending the Global Mass Change Data Record: GRACE Follow-On Instrument and Science Data Performance. *Geophysical Research Letters* **2020**, 47(12), e2020GL088306. <https://doi.org/10.1029/2020GL088306>.
- ¹⁴ Boergens, E.; Güntner, A.; Dobsław, H. et al. Quantifying the Central European Droughts in 2018 and 2019 With GRACE Follow-On. *Geophysical Research Letters* **2020**, 47(14), e2020GL087285. <https://doi.org/10.1029/2020GL087285>.
- ¹⁵ EM-DAT, CRED/UCLouvain, Brussels, Belgium. <http://www.emdat.be>.
- ¹⁶ The findings presented in this section are from the *WMO State of the Global Climate 2022* (WMO-No. 1316).
- ¹⁷ Lehner, B.; Verdin, K.; Jarvis, A. New Global Hydrography Derived from Spaceborne Elevation Data. *Eos, Transactions American Geophysical Union* **2008**, 89(10), 93–94. <https://doi.org/10.1029/2008EO100001>.
- ¹⁸ Hanazaki, R.; Yamazaki, D.; Yoshimura, K. Development of a Reservoir Flood Control Scheme for Global Flood Models. *Journal of Advances in Modeling Earth Systems* **2022**, 14(3), e2021MS002944. <https://doi.org/10.1029/2021MS002944>.
- ¹⁹ Yamazaki, D.; Kanae, S.; Kim, H. et al. A Physically Based Description of Floodplain Inundation Dynamics in a Global River Routing Model. *Water Resources Research* **2011**, 47(4). <https://doi.org/10.1029/2010WR009726>.
- ²⁰ Yuan, X.; Ji, P.; Wang, L. et al. High-Resolution Land Surface Modeling of Hydrological Changes Over the Sanjiangyuan Region in the Eastern Tibetan Plateau: 1. Model Development and Evaluation. *Journal of Advances in Modeling Earth Systems* **2018**, 10(11), 2806–2828. <https://doi.org/10.1029/2018MS001412>.
- ²¹ van Verseveld, W. J.; Weerts, A. H.; Visser, M. et al. Wflow_sbm v0.6.1, a Spatially Distributed Hydrologic Model: From Global Data to Local Applications. *Geoscientific Model Development Discussions* **2022**, 1–52. <https://doi.org/10.5194/gmd-2022-182>.



- ²² Imhoff, R. O.; van Verseveld, W. J.; van Osnabrugge, B. et al. Scaling Point-Scale (Pedo)Transfer Functions to Seamless Large-Domain Parameter Estimates for High-Resolution Distributed Hydrologic Modeling: An Example for the Rhine River. *Water Resources Research* **2020**, *56* (4), e2019WR026807. <https://doi.org/10.1029/2019WR026807>.
- ²³ Eilander, D.; van Verseveld, W.; Yamazaki, D. et al. A Hydrography Upscaling Method for Scale-Invariant Parametrization of Distributed Hydrological Models. *Hydrology and Earth System Sciences* **2021**, *25* (9), 5287–5313. <https://doi.org/10.5194/hess-25-5287-2021>.
- ²⁴ Murray, A. M.; Jørgensen, G. H.; Godiksen, P. N. et al. DHI-GHM: Real-Time and Forecasted Hydrology for the Entire Planet. *Journal of Hydrology* **2023**, *620*, 129431. <https://doi.org/10.1016/j.jhydrol.2023.129431>.
- ²⁵ Alfieri, L.; Burek, P.; Dutra, E. et al. GloFAS – Global Ensemble Streamflow Forecasting and Flood Early Warning. *Hydrology and Earth System Sciences* **2013**, *17* (3), 1161–1175. <https://doi.org/10.5194/hess-17-1161-2013>.
- ²⁶ Grimaldi, S.; Salamon, P.; Disperati, J. et al. (2022): GloFAS v4.0 Hydrological Reanalysis; European Commission, Joint Research Centre (JRC) [Dataset]. <http://data.europa.eu/89h/f96b7a19-0133-4105-a879-0536991ca9c5>.
- ²⁷ Boussetta, S.; Balsamo, G.; Arduini, G. et al. ECLand: The ECMWF Land Surface Modelling System. *Atmosphere* **2021**, *12* (6), 723. <https://doi.org/10.3390/atmos12060723>.
- ²⁸ Samaniego, L.; Kumar, R.; Attinger, S. Multiscale Parameter Regionalization of a Grid-Based Hydrologic Model at the Mesoscale. *Water Resources Research* **2010**, *46* (5). <https://doi.org/10.1029/2008WR007327>.
- ²⁹ Kumar, R.; Samaniego, L.; Attinger, S. Implications of Distributed Hydrologic Model Parameterization on Water Fluxes at Multiple Scales and Locations. *Water Resources Research* **2013**, *49* (1), 360–379. <https://doi.org/10.1029/2012WR012195>.
- ³⁰ Samaniego, L.; Kaluza, M.; Kumar, R. et al. Mesoscale Hydrologic Model, 2019. <https://doi.org/10.5281/zenodo.3239055>.
- ³¹ Nie, W.; Kumar, S. V.; Getirana, A. et al. Nonstationarity in the Global Terrestrial Water Cycle and its Interlinkages in the Anthropocene. *Research Square* **2023** [preprint]. <https://www.researchsquare.com/article/rs-3168072/v1.pdf>.
- ³² *A Global Reanalysis for Water, Energy, and Carbon Cycle Variables Overview*. <https://www.earthdata.nasa.gov/dashboard/data-catalog/global-reanalysis-da>.
- ³³ Yoshimura, K.; Sakimura, T.; Oki, T. et al. Toward Flood Risk Prediction: A Statistical Approach Using a 29-Year River Discharge Simulation over Japan. *Hydrological Research Letters* **2008**, *2*, 22–26. <https://doi.org/10.3178/hrl.2.22>.
- ³⁴ Ma, W.; Ishitsuka, Y.; Takeshima, A. et al. Applicability of a Nationwide Flood Forecasting System for Typhoon Hagibis 2019. *Sci Rep* **2021**, *11* (1), 10213. <https://doi.org/10.1038/s41598-021-89522-8>.
- ³⁵ Müller Schmied, H.; Cáceres, D.; Eisner, S. et al. The Global Water Resources and Use Model WaterGAP v2.2d: Model Description and Evaluation. *Geoscientific Model Development* **2021**, *14* (2), 1037–1079. <https://doi.org/10.5194/gmd-14-1037-2021>.
- ³⁶ Müller Schmied, H.; Cáceres, D.; Eisner, S. et al. The Global Water Resources and Use Model WaterGAP v2.2d: Model Description and Evaluation. *Geoscientific Model Development* **2021**, *14* (2), 1037–1079. <https://doi.org/10.5194/gmd-14-1037-2021>.
- ³⁷ Arheimer, B.; Pimentel, R.; Isberg, K. et al. Global Catchment Modelling Using World-Wide HYPE (WWH), Open Data, and Stepwise Parameter Estimation. *Hydrology and Earth System Sciences* **2020**, *24* (2), 535–559. <https://doi.org/10.5194/hess-24-535-2020>.
- ³⁸ All river discharge data from GRDC and most from the Member States and Territories were quality-controlled.
- ³⁹ Global Runoff Data Centre (GRDC). *WMO Basins and Sub-Basins*; 3rd rev. ext. ed., Federal Institute of Hydrology (BfG): Koblenz, Germany, 2020.
- ⁴⁰ Zanchetin, D. *Monthly Discharge of Po River at Pontelagoscuro*, 2022. <https://doi.org/10.5281/zenodo.7225699>.
- ⁴¹ Montanari, A.; Nguyen, H.; Rubinetti, S. et al. Why the 2022 Po River Drought Is the Worst in the Past Two Centuries. *Science Advances* **2023**, *9* (32), eadg8304. <https://doi.org/10.1126/sciadv.adg8304>.
- ⁴² The river discharge rankings from simulated and observed data for the year 2022 were classified by the sign of change with respect to the long-term normal (as described in Box 1) and then compared. Hatching in Figure A6 of Annex 1, shows basins where the GHMS simulations agreed with the observed data.



- ⁴³ At the global scale, river discharge conditions in 2021 followed a similar pattern, with more area experiencing drier-than-usual conditions compared to areas with wetter-than-usual conditions. In 2022, more area globally was drier than near-normal conditions than in 2021. (Note that due to finer basin delineation adopted in 2022, the results for 2021 cannot be quantitatively compared to those from 2022.)
- ⁴⁴ Naumann, G.; Podestá, G.; Marengo, J., et al. *Extreme and Long-term Drought in the La Plata Basin: Event Evolution and Impact Assessment until September 2022*; JRC132245; Publications Office of the European Union: Luxembourg, 2023. <https://doi.org/10.2760/62557>.
- ⁴⁵ Muñoz, S. E.; Dee, S. G.; Luo, X. et al. Mississippi River Low-Flows: Context, Causes, and Future Projections. *Environ. Res.: Climate* **2023**, 2(3), 031001. <https://doi.org/10.1088/2752-5295/acd8e3>.
- ⁴⁶ <https://www.lwcb.ca/permpdf/Reporton2022FloodinginWRBasin.pdf>
- ⁴⁷ <https://earthobservatory.nasa.gov/images/150712/worst-drought-on-record-parches-horn-of-africa>
- ⁴⁸ Note that the Horn of Africa predominantly experiences two precipitation seasons per year, one in March–April–May and one in October–November–December.
- ⁴⁹ <https://www.worldweatherattribution.org/human-induced-climate-change-increased-drought-severity-in-southern-horn-of-africa/>
- ⁵⁰ <https://www.worldweatherattribution.org/methodological-papers/>
- ⁵¹ <https://earthobservatory.nasa.gov/images/150712/worst-drought-on-record-parches-horn-of-africa>
- ⁵² <https://climate.copernicus.eu/seasonal-review-europes-record-breaking-summer>
- ⁵³ https://www.esa.int/ESA_Multimedia/Images/2022/08/Drought_causes_Yangtze_to_shrink
- ⁵⁴ Ma, M.; Qu, Y.; Lyu, J. et al. The 2022 Extreme Drought in the Yangtze River Basin: Characteristics, Causes and Response Strategies. *River* **2022**, 1(2), 162–171. <https://doi.org/10.1002/rvr2.23>.
- ⁵⁵ <https://www.globalwaterwatch.earth/>
- ⁵⁶ van Verseveld, W. J.; Weerts, A. H.; Visser, M. et al. Wflow_sbm v0.6.1, a Spatially Distributed Hydrologic Model: From Global Data to Local Applications. *Geoscientific Model Development Discussions* **2022**, 1–52. <https://doi.org/10.5194/gmd-2022-182>.
- ⁵⁷ Hanazaki, R.; Yamazaki, D.; Yoshimura, K. Development of a Reservoir Flood Control Scheme for Global Flood Models. *Journal of Advances in Modeling Earth Systems* **2022**, 14(3), e2021MS002944. <https://doi.org/10.1029/2021MS002944>.
- ⁵⁸ Yamazaki, D.; Kanae, S.; Kim, H. et al. A Physically Based Description of Floodplain Inundation Dynamics in a Global River Routing Model. *Water Resources Research* **2011**, 47(4). <https://doi.org/10.1029/2010WR009726>.
- ⁵⁹ Arheimer, B.; Pimentel, R.; Isberg, K. et al. Global Catchment Modelling Using World-Wide HYPE (WWH), Open Data, and Stepwise Parameter Estimation. *Hydrology and Earth System Sciences* **2020**, 24(2), 535–559. <https://doi.org/10.5194/hess-24-535-2020>.
- ⁶⁰ Lehner, B.; Reidy Liermann, C.; Revenga, C. et al. *Global Reservoir and Dam Database, Version 1 (GRanDv1): Dams*, Revision 01; NASA Socioeconomic Data and Applications Center (SEDAC): Palisades, USA, 2011. <https://doi.org/10.7927/H4N877QK>.
- ⁶¹ Note the discrepancy in the patterns between Figures 3 and 4 for this region.
- ⁶² Duran-Llacer, I.; Munizaga, J.; Arumí, J. L. et al. Lessons to Be Learned: Groundwater Depletion in Chile’s Ligua and Petorca Watersheds through an Interdisciplinary Approach. *Water* **2020**, 12(9), 2446. <https://doi.org/10.3390/w12092446>.
- ⁶³ Hirata, R.; Foster, S. The Guarani Aquifer System – from Regional Reserves to Local Use. *Quarterly Journal of Engineering Geology and Hydrogeology* **2021**, 54(1), qjgh2020-091. <https://doi.org/10.1144/qjgh2020-091>.
- ⁶⁴ <http://www.bom.gov.au/climate/current/annual/aus/#tabs=Water>
- ⁶⁵ https://www.dws.gov.za/Groundwater/maps/gwlevelmaps2015_2021.aspx
- ⁶⁶ <https://www.brgm.fr/en/news/press-release/groundwater-tables-1-march-2023>



- ⁶⁷ McGuire, V. L. *Water-Level and Recoverable Water in Storage Changes, High Plains Aquifer, Predevelopment to 2015 and 2013–15*; Scientific Investigations Report 2017–5040; United States Geological Survey: Reston, USA, 2017. <https://pubs.usgs.gov/sir/2017/5040/sir20175040.pdf>.
- ⁶⁸ <https://www.eea.europa.eu/ims/soil-moisture-deficit>
- ⁶⁹ <https://gcos.wmo.int/en/essential-climate-variables/soil-moisture>
- ⁷⁰ Nie, W.; Kumar, S. V.; Getirana, A. et al. Nonstationarity in the Global Terrestrial Water Cycle and its Interlinkages in the Anthropocene. *Research Square* **2023** [preprint]. <https://www.researchsquare.com/article/rs-3168072/v1.pdf>.
- ⁷¹ *A Global Reanalysis for Water, Energy, and Carbon Cycle Variables Overview*. <https://www.earthdata.nasa.gov/dashboard/data-catalog/global-reanalysis-da>.
- ⁷² Kumar, S. V.; Peters-Lidard, C. D.; Tian, Y. et al. Land Information System: An Interoperable Framework for High Resolution Land Surface Modeling. *Environmental Modelling & Software* **2006**, *21* (10), 1402–1415. <https://doi.org/10.1016/j.envsoft.2005.07.004>.
- ⁷³ Kumar, S. V.; Mocko, D. M.; Wang, S. et al. Assimilation of Remotely Sensed Leaf Area Index into the Noah-MP Land Surface Model: Impacts on Water and Carbon Fluxes and States over the Continental United States. *Journal of Hydrometeorology* **2019**, *20* (7), 1359–1377. <https://doi.org/10.1175/JHM-D-18-0237.1>.
- ⁷⁴ <https://climate.copernicus.eu/esotc/2022/drought>
- ⁷⁵ Nie, W.; Kumar, S. V.; Getirana, A. et al. Nonstationarity in the Global Terrestrial Water Cycle and its Interlinkages in the Anthropocene. *Research Square* **2023** [preprint]. <https://www.researchsquare.com/article/rs-3168072/v1.pdf>.
- ⁷⁶ Nanditha, J. S.; Kushwaha, A. P.; Singh, R. et al. The Pakistan Flood of August 2022: Causes and Implications. *Earth's Future* **2023**, *11* (3), e2022EF003230. <https://doi.org/10.1029/2022EF003230>.
- ⁷⁷ Landerer, F. W.; Flechtner, F. M.; Save, H. et al. Extending the Global Mass Change Data Record: GRACE Follow-On Instrument and Science Data Performance. *Geophysical Research Letters* **2020**, *47*(12), e2020GL088306. <https://doi.org/10.1029/2020GL088306>.
- ⁷⁸ Boergens, E.; Güntner, A.; Dobslaw, H. et al. Quantifying the Central European Droughts in 2018 and 2019 With GRACE Follow-On. *Geophysical Research Letters* **2020**, *47*(14), e2020GL087285. <https://doi.org/10.1029/2020GL087285>.
- ⁷⁹ The Smart & Precise Prognostic Hydrology in Central Asia (SAPPHIRE Central Asia) is an initiative developed to support the Central Asian National Hydrological and Meteorological Services in utilizing data from modern automatic or remote monitoring technologies. It operationalizes the use of cryosphere data by providing a basin-scale snow tracker representing the real-time analysis of snow water equivalent against climatic averages to identify anomalies over the region (see Figure 15).
- ⁸⁰ Mudryk, L.; Elias Chereque, A.; Derksen, C. et al. *Arctic Report Card 2022: Terrestrial Snow Cover*. <https://doi.org/10.25923/yxs5-6c72>.
- ⁸¹ EM-DAT, CRED/UCLouvain, Brussels, Belgium. <http://www.emdat.be>.
- ⁸² <https://www.worldbank.org/en/news/press-release/2022/10/28/pakistan-flood-damages-and-economic-losses-over-usd-30-billion-and-reconstruction-needs-over-usd-16-billion-new-assessme>
- ⁸³ World Meteorological Organization (WMO). *State of the Global Climate 2022* (WMO-No. 1316). Geneva, 2023.
- ⁸⁴ Nanditha, J. S.; Kushwaha, A. P.; Singh, R. et al. The Pakistan Flood of August 2022: Causes and Implications. *Earth's Future* **2023**, *11* (3), e2022EF003230. <https://doi.org/10.1029/2022EF003230>.
- ⁸⁵ <https://www.worldweatherattribution.org/climate-change-likely-increased-extreme-monsoon-rainfall-flooding-highly-vulnerable-communities-in-pakistan/>
- ⁸⁶ <https://reliefweb.int/report/pakistan/wfp-pakistan-floods-situation-report-13-february-2023>
- ⁸⁷ World Meteorological Organization (WMO). *State of the Global Climate 2022* (WMO-No. 1316). Geneva, 2023.
- ⁸⁸ <https://reliefweb.int/report/pakistan/ndma-monsoon-2022-daily-situation-report-no-115-dated-6th-oct-2022>
- ⁸⁹ <https://reliefweb.int/report/pakistan/ndma-monsoon-2022-daily-situation-report-no-129-dated-20th-oct-2022>



- ⁹⁰ <https://www.worldbank.org/en/news/press-release/2022/10/28/pakistan-flood-damages-and-economic-losses-over-usd-30-billion-and-reconstruction-needs-over-usd-16-billion-new-assessme>
- ⁹¹ <https://www.undp.org/sites/g/files/zskgke326/files/2022-12/Pakistan%20PDNA%20Main%20Report%20-%20Final.pdf>
- ⁹² EM-DAT, CRED/UCLouvain, Brussels, Belgium. <http://www.emdat.be>.
- ⁹³ World Meteorological Organization (WMO). *State of the Global Climate 2022* (WMO-No. 1316). Geneva, 2023.
- ⁹⁴ EM-DAT, CRED/UCLouvain, Brussels, Belgium. <http://www.emdat.be>.
- ⁹⁵ World Meteorological Organization (WMO). *State of the Global Climate 2022* (WMO-No. 1316). Geneva, 2023.
- ⁹⁶ [https://www.unicef.org/media/130026/file/Nigeria%20Flash%20Update%20\(Flood\)%20for%20September%20%E2%80%93%20November%202022.pdf](https://www.unicef.org/media/130026/file/Nigeria%20Flash%20Update%20(Flood)%20for%20September%20%E2%80%93%20November%202022.pdf)
- ⁹⁷ World Meteorological Organization (WMO). *State of the Global Climate 2022* (WMO-No. 1316). Geneva, 2023.
- ⁹⁸ <https://earthobservatory.nasa.gov/images/150712/worst-drought-on-record-parches-horn-of-africa#:~:text=As%20the%20end%20of%202022,raise%20livestock%2C%20and%20buy%20food>
- ⁹⁹ <https://reliefweb.int/report/ethiopia/horn-africa-drought-regional-humanitarian-overview-call-action-revised-21-september-2022>
- ¹⁰⁰ <https://reliefweb.int/report/ethiopia/horn-africa-drought-regional-humanitarian-overview-call-action-revised-21-september-2022>
- ¹⁰¹ <https://www.unicef.org/press-releases/more-twenty-million-children-suffering-horn-africa-drought-intensifies-unicef>
- ¹⁰² Naumann, G.; Podestá, G.; Marengo, J., et al. *Extreme and Long-term Drought in the La Plata Basin: Event Evolution and Impact Assessment until September 2022*; JRC132245; Publications Office of the European Union: Luxembourg, 2023. <https://doi.org/10.2760/62557>.
- ¹⁰³ World Meteorological Organization (WMO). *State of the Climate in Latin America and the Caribbean 2022* (WMO-No. 1322). Geneva, 2023.
- ¹⁰⁴ World Meteorological Organization (WMO). *State of the Global Climate 2022* (WMO-No. 1316). Geneva, 2023.
- ¹⁰⁵ Montanari, A.; Nguyen, H.; Rubinetti, S. et al. Why the 2022 Po River Drought Is the Worst in the Past Two Centuries. *Science Advances* **2023**, *9* (32), eadg8304. <https://doi.org/10.1126/sciadv.adg8304>.
- ¹⁰⁶ <https://www.nature.com/articles/d43978-022-00089-y>
- ¹⁰⁷ World Meteorological Organization (WMO). *State of the Global Climate 2022* (WMO-No. 1316). Geneva, 2023.
- ¹⁰⁸ <https://www.ceh.ac.uk/news-and-media/blogs/dry-weather-and-heatwave-put-increased-pressure-uk-water-resources>
- ¹⁰⁹ <https://www.ceh.ac.uk/news-and-media/blogs/dry-weather-and-heatwave-put-increased-pressure-uk-water-resources>
- ¹¹⁰ Matthias Huss, based on Glacier Monitoring Switzerland (GLAMOS). Swiss Glacier Mass Balance; Release 2022; GLAMOS. <https://doi.org/10.18750/massbalance.2022.r2022>.
- ¹¹¹ More detailed information about these models and their agreement can be found in the Annex 1 of the report.
- ¹¹² Stahl, K.; Weiler, M.; van Tiel, M. *Impact of Climate Change on the Rain, Snow and Glacier Melt Components of Streamflow of the River Rhine and Its Tributaries*; CHR Report No. I-28; International Commission for the Hydrology of the Rhine Basin: Lelystad, Netherlands, 2022. https://www.chr-khr.org/sites/default/files/ASG-II_Synthese_EN_mit-Links.pdf.
- ¹¹³ See, for example, Shukla, S.; Sheffield, J.; Wood, E. F.; Lettenmaier, D. P. On the Sources of Global Land Surface Hydrologic Predictability. *Hydrology and Earth System Sciences* **2013**, *17* (7), 2781–2796. <https://doi.org/10.5194/hess-17-2781-2013>.

Annex 1. Technical annex

This Annex provides high-level information on the main methodological steps applied to portray the state of global water resources in the year 2022.

METHODS

For the *State of Global Water Resources 2022* report, the resolution of primary hydrological basins was increased, resulting in 986 basins spanning the globe. The basin map was based on Hydrobasins level 4 data.¹ The original dataset contained about 1 300 basins. However, due to global hydrological modelling system (GHMS) resolution, basins with a drainage area of less than 10 000 km² were filtered out together with some regions (such as Greenland) leaving 986 basins (Figure A1).

DATA SOURCES

Several sources of information on water resources were used to produce this report — in particular the following:

- Observed river discharge data were obtained from the respective National Hydrological and Meteorological Services (NHMSs) of countries and the Global Runoff Data Centre (GRDC).^{2,3}
- Simulated river discharge data were obtained from several GHMSs. For more information on the models used, please refer to the [Global hydrological modelling systems](#) section of this Annex.
- Inflow into selected reservoirs globally was obtained from the Wflow_sbm,⁴ CaMa-Flood⁵ and WWH models.⁶
- The global terrestrial water storage (TWS) anomaly was obtained from the GRACE project.^{7,8}

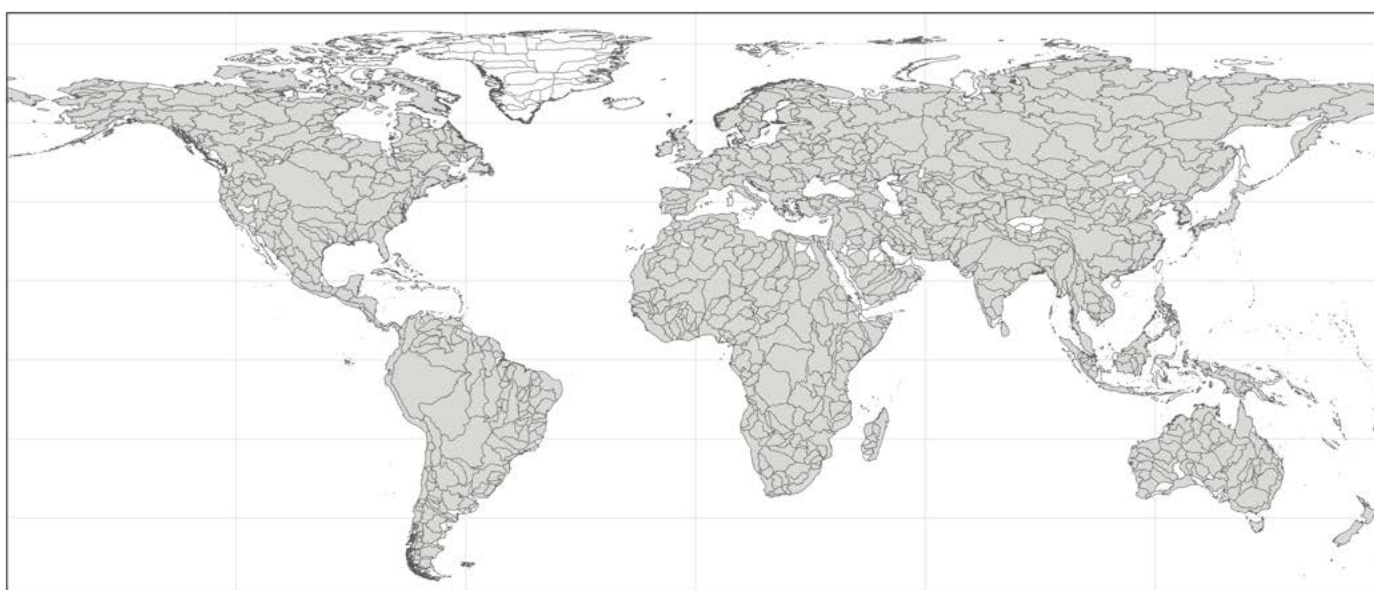


Figure A1. Global coverage of selected hydrological basins



- Qualitative and quantitative information on high-impact events was obtained from open data sources, such as the EM-DAT database,⁹ ReliefWeb, WMO State of the Climate reports and others.
- Observed groundwater data were obtained from the International Groundwater Resources Assessment Centre (IGRAC) for the selected 10 countries.
- Soil moisture and evapotranspiration data were obtained from the global water cycle reanalysis product NASA-LISF-Noah MP.¹⁰
- Data on glaciers were received from WMO Member States and Territories and external experts.

VARIABLE RANKING

In order to provide a coherent picture across the different data sets obtained, the same method of variable ranking was applied to the variables listed in the previous section: discharge, inflow into reservoirs, soil moisture, evapotranspiration, groundwater levels and TWS.

Averages over historical periods from modelled and observed data sets were calculated for each year. The resulting array was ranked, and the yearly average of a selected variable for the year 2022 was then compared to this ranked array and classified according to the following rule:

much below normal:	$Q_{2022} \leq 10\text{th percentile}$
below normal:	$10\text{th percentile} < Q_{2022} < 25\text{th percentile}$
normal:	$25\text{th} \leq Q_{2022} \leq 75\text{th percentile}$
above normal:	$75\text{th} < Q_{2022} < 90\text{th percentile}$
much above normal:	$Q_{2022} \geq 90\text{th percentile}$

The historical period varied depending on the variable in question, and was constrained by the data availability. Refer to Table A1 for selected historical periods and to data set-specific Chapters of the main report for more details.

Table A1. Historical periods of selected data sets

<i>Data set</i>	<i>Selected historical period</i>	<i>Length of historical period</i>
Simulated discharge from GHMs	1991–2020 ^a	30 years
Observed discharge from GRDC and GHMSs	<2001–2020	Varies between 20 and 30 years
Inflow into reservoirs	1991–2020	30 years
Evapotranspiration	2003–2020	18 years
Soil moisture	2003–2020	18 years
Groundwater	2013–2022	10 years
TWS	2002–2020	19 years

^a For some GHMSs the simulation period was available only to 2003–2022. In this case results were used only for the model intercomparison.



For the modelled data, where several data sources (ensemble of models) have been used (specifically, for inflow into reservoirs and discharge data from GHMSs), the averaging of the variable ranking results was done at the basin level. For each model in the ensemble, the above-specified rankings were assigned an integer (“much below normal” = 1, “below normal” = 2, “normal” = 3, “above normal” = 4, “much above normal” = 5), and then an average was calculated across the ensemble of models for each of the basins. The resulting number was rounded, and the average discharge ranking was derived for each basin, according to the thresholds listed above.

RIVER DISCHARGE

GLOBAL HYDROLOGICAL MODELLING SYSTEMS

The 2022 report predominantly uses outcomes from the GHMSs sourced from the modelling community. Despite improved availability, observed discharge data were still not sufficient to ensure a consistent global overview, requiring an alternative source for discharge data. The simulated discharge produced by multiple GHMSs was analysed using the subbasin map obtained after processing the level 4 Hydrobasins data set (Figure A1).

In total, 11 GHMSs were used in the modelling exercise:

- World-wide HYPE (WWH) v1.3.9;¹¹
- WaterGAP 2.2e;^{12,13}
- Conjunctive Surface–Subsurface Process, version 2 (CSSPv2);¹⁴
- Mesoscale Hydrologic Model (mHM);^{15,16,17}
- DHI-GHM;¹⁸
- CaMa-Flood with Dam;^{19,20}
- Today’s Earth – Global (TEJRA55);^{21,22}
- Global Flood Awareness System (GloFAS);^{23,24}
- The European Centre for Medium-Range Weather Forecasts (ECMWF) Land Surface Modelling System ECLand;²⁵
- NASA-LISF-Noah MP;²⁶
- Wflow_sbm.^{27,28,29}

It was not possible to include the simulations provided from the CRHM model³⁰ due to the temporal and spatial limits of the model.

The global hydrological modelling community was asked to provide historical simulations for the chosen 986 basins for the years 1991–2020 and the target year of 2022, using meteorological input data of their choice. Before submitting the outputs, the modelling teams were required to complete a modelling dictionary, offering necessary technical details about the model and input data sources. An ensemble of models was employed to address potential uncertainties in the simulations. The 2022 discharge ranking was conducted initially for the simulated discharge from each model for each basin, then averaged across all models for each basin (refer to the [Variable ranking](#) section for more details).

Table A2 shows a technical breakdown of the various GHMSs, and the [Validation of modelled results](#) chapter summarizes the models’ spatial coverage and provides a graphical representation of trends simulated by each model for each basin. Due to time restrictions, it was not feasible to homogenize input data sources for model setup across all modelling groups. Regarding climate forcing, all GHMSs used ERA5 reanalysis data,³¹ except for the WWH and TEJRA55 models, which were driven by the HydroGFD³² and JRA-55³³ data sets, respectively.



Table A2. Characteristics of global hydrological modelling systems used in the report

<i>Model name</i>	<i>Institution</i>	<i>Spatial coverage</i>	<i>Spatial model resolution</i>	<i>Climate data product used</i>	<i>Simulations used in the report</i>
WaterGAP 2.2e	Goethe University Frankfurt	Global	0.5° × 0.5°	20CRv3-ERA5	main report: streamflow simulations
Conjunctive Surface–Subsurface Process version 2 (CSSPv2)	Nanjing University of Information Science and Technology	Global	0.125°–0.25°	ERA5	additional analysis: streamflow simulations
Mesoscale Hydrologic Model (mHM)	Helmholtz Centre for Environmental Research – UFZ	Two setups available: (i) global and (ii) individually delineated and calibrated GRDC basins	Last version was based on the 0.25° resolution	ERA5	main report: streamflow simulations
World-Wide HYPE (WWH) version 1.3.9	Swedish Meteorological and Hydrological Institute	All continents except Antarctica	On average 1 000 km ²	HydroGFD	main report: streamflow simulations/ reservoirs
DHI-GHM	DHI	Covers land surface of the globe between 60°S and 80°N	0.1° × 0.1°	ERA5	main report: streamflow simulations
CaMa-Flood with Dam	University of Tokyo	60°S–90°N, 180°W–180°E (not including Greenland)	0.25° lat./lon. deg.	ERA5-land runoff	main report: streamflow simulations/ reservoirs
Today’s Earth –Global (TEJRA55)	University of Tokyo/Japan Aerospace Exploration Agency	60°S–90°N, 180°W–180°E (not including Greenland)	0.25° lat./lon. deg.	JRA-55	main report: streamflow simulations
Global Flood Awareness System (GloFAS)	European Commission Joint Research Centre (JRC)	Global except for Antarctica (60°S–90°N, 180°W–180°E)	0.05° (~5 km, gridded)	ERA5	main report: streamflow simulations



<i>Model name</i>	<i>Institution</i>	<i>Spatial coverage</i>	<i>Spatial model resolution</i>	<i>Climate data product used</i>	<i>Simulations used in the report</i>
The ECMWF Land Surface Modelling System (ECLand)	European Centre for Medium-Range Weather Forecasts (ECMWF)	Global	or 15 arcmin (0.25°, ~25 km)	ERA5	main report: streamflow simulations
NASA-LISF-Noah MP	NASA	Global	10 km	NASA MERRA2	main report: soil moisture, ET, Annex: streamflow simulations inter model comparison
Wflow_sbm	Deltares	Global	30 arcsec (0.0083° ~1 km)	ERA5	main report: reservoirs, streamflow simulations (Europe only)
CRHM	Cold Regions Hydrological Modelling platform (CRHM)	Regional	HRU		Due to short simulation period it was not used in the simulation exercise

Simulations for streamflow from the NASA-LISF-Noah MP model were used solely for model intercomparison and not for the 2022 assessment of water resources. The data only covered the period from 2003 to 2022, and the ranking obtained from the results differed from the average of the model ensemble means (this might be due to the difference in reference period). Similarly, the CSSPv2 model was also used only for model comparison and to validate results, as the data were only available for GRDC stations. In addition, it was not possible to include results from the CRHM model due to the limited number of stations and because the simulation period did not extend to the year 2022.

OBSERVED DATA AND VALIDATION OF MODELLED RESULTS

General discharge data availability from GRDC and NHMSs for 2022

Observed discharge data were obtained from the GRDC and received from the NHMSs. Two selection criteria were adjusted to increase the potential volume of observed data: the historical period was permitted to span a minimum of 20 years, instead of 30 as for the modelled data, and data sets not yet subjected to quality checks were included (this was the case only for the United Kingdom data set from October–December 2022).

In total, observed data from nearly 500 stations for the year 2022 were collected from the GRDC database and NHMSs. Two subsets were derived from this total pool for further detailed analysis. The first subset, consisting of 273 stations, with a maximum of 20 days of missing data in 2022, was selected for evaluating the 2022 discharge anomaly. The second subset, comprising 91 stations, was identified for validating the GHMSs' results. These stations were selected from the 273 stations based on their proximity to the chosen basin outlet, ensuring a closer match between the observed and modelled data.

Figure A2 presents the locations of the 273 gauges selected for discharge anomaly analysis for 2022 and the 91 selected for validation of modelling results, including the basins where those were located. Note that the ranking of the streamflow for 2022 estimated from the ensemble

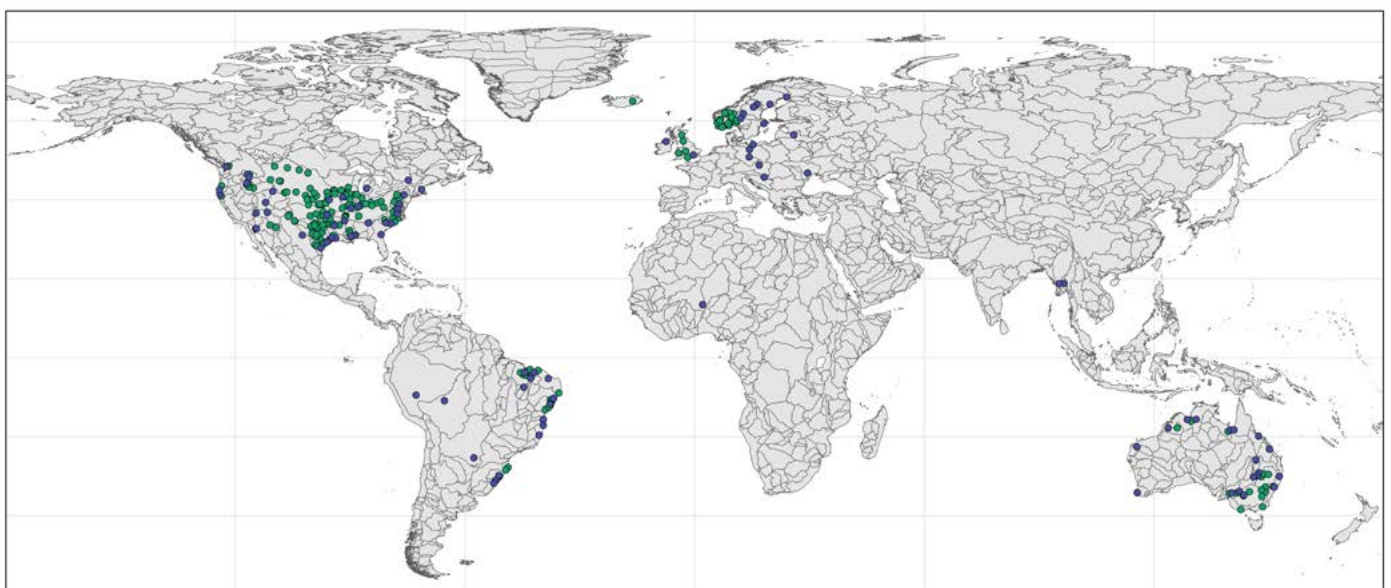


Figure A2. Location of the gauges selected in the GRDC database and for which data were received from NHMSs (green points), and those selected for validation (blue points), along with the respective basins, where those gauges were located (blue points).

of GHMSs might differ from the results obtained from the observed streamflow data at a finer spatial scale. Therefore, WMO emphasizes the importance of availability of local in situ data for producing accurate global products such as the assessments presented in this report.

Figure A3 presents discharge ranking results obtained for each of the basins from 10 GHMSs. The CSSPv2 model has been used only for validation of results from the GRDC database. The simulation period for the NASA-LISF-Noah MP model was limited to 2003–2022, and this model has been used only for comparison with other GHMSs. The results from the Wflow_sbm model are presented only for Europe.

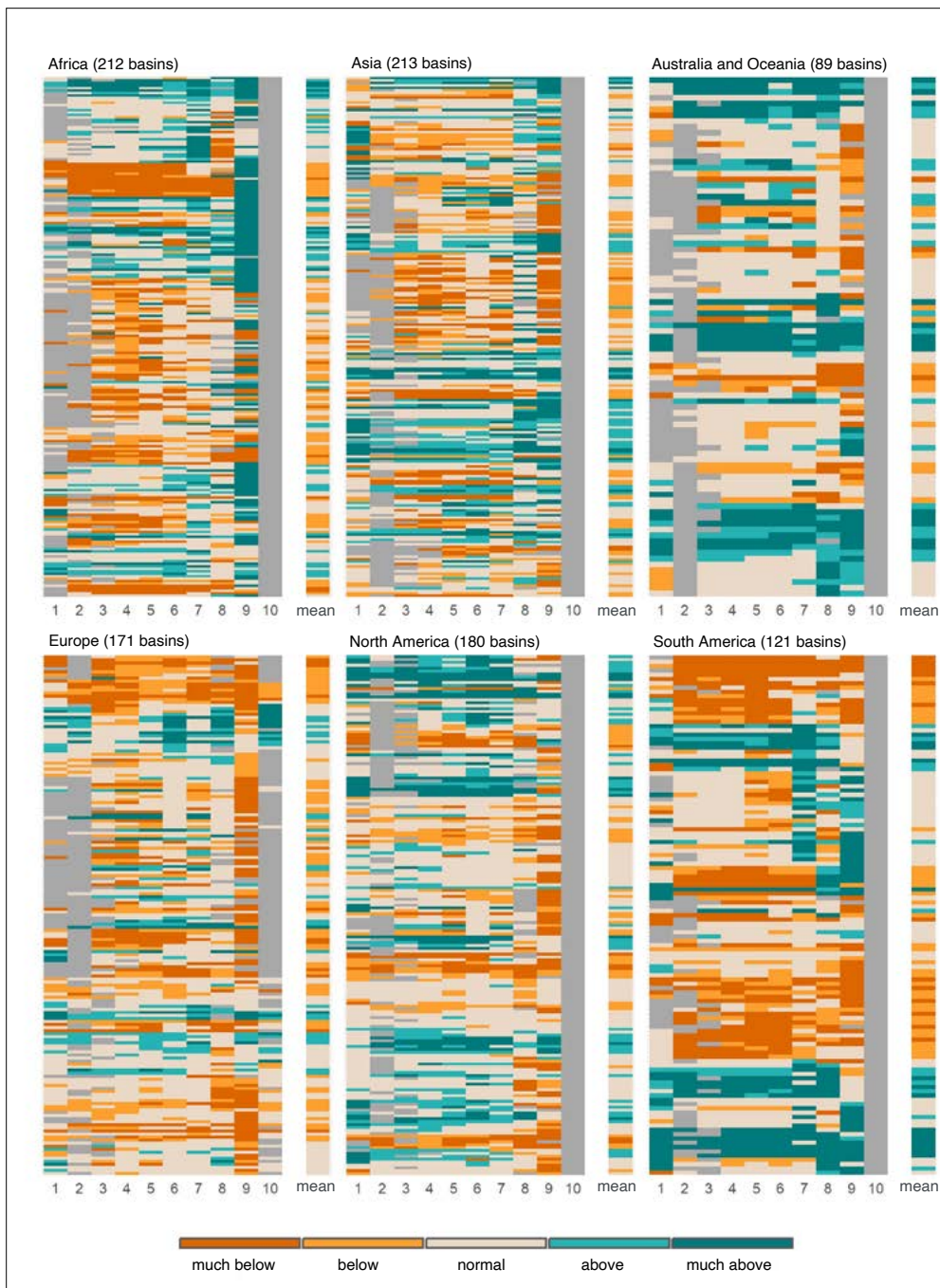


Figure A3. Simulated discharge rankings for the year 2022 for each basin by each of the GHMSs grouped by region.

Note: 1 – TEJRA55,
 2 – mHM,
 3 – CaMa-Flood,
 4 – ECLand,
 5 – GloFAS,
 6 – WaterGAP 2.2e,
 7 – DHI-GHM,
 8 – WWH,
 9 – NASA-LISF-Noah MP,
 10 – Wflow; grey area indicates no data values for a specific basin.

Validation of modelled results

The discharge ranking obtained from the GHMS simulations was validated with discharge ranking obtained from the available observed data. Annual averages of flow observations from 2022 were ranked against the hydrological normals (obtained from at least 20 years of flow observations) for each WMO basin (where observed flow data were available). The discharge rankings from simulated and observed data for the year 2022 were classified by the sign of change with respect to the long-term normal (that is, “below”, “above” or “normal”) and then compared to each other. Those basins where agreement was found between the GHMS simulations and observed data are indicated through the hatching of the basins (Figure A6).

Note that in large basins where some of the downstream units (according to the WMO basin classification) import a considerable amount of water resources from the upstream catchments, comparisons/validations done between results from modelled data and observations for only one gauge per WMO basin might lead to inaccurate results. Therefore, using observations from intermediary gauges or redefining of the catchment areas must be considered in the future to minimize uncertainties in the results.

Figure A4 shows model agreement on the sign of changes among GHMSs used in the simulation task for each basin. The results show that more than 50% of GHMSs agree on the sign of trends for 94% of the area globally. Moreover, the agreement for Australia, North and South America is between 75% and 100% for more than 65% of the area.

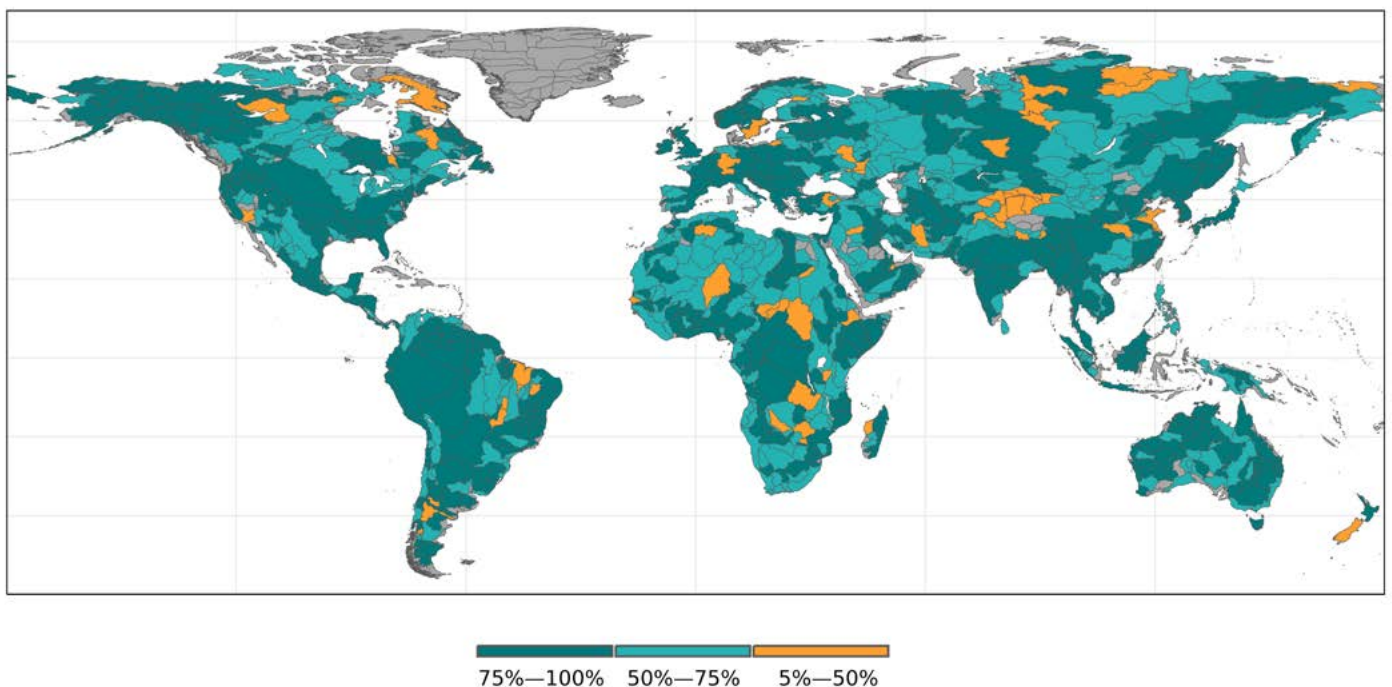


Figure A4. Share of GHMSs that agree on the sign of changes for each basin

Figure A5 presents observed discharge anomaly for the year 2022 for selected basins. Figure A6 shows validation of trend simulations for the 2022 discharge. Areas where simulated and observed trends agree on the direction of change are indicated by hatching.

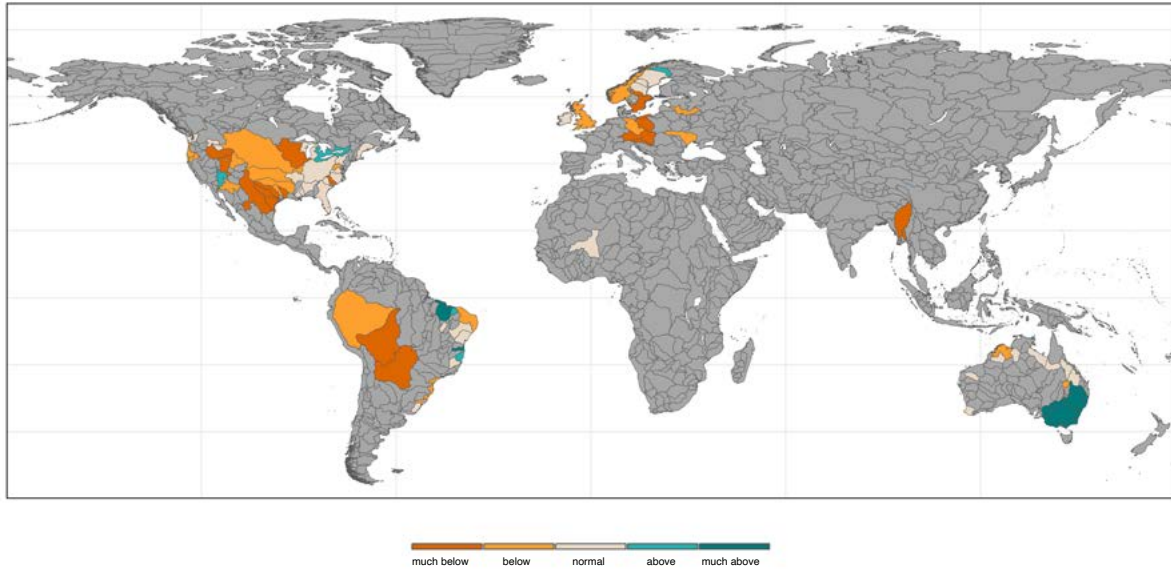


Figure A5. River discharge in 2022 as ranked with respect to the historical period 1991–2020. The results presented here were derived from the observed discharge data, which were obtained from GHMSs and the GRDC database. Grey areas indicate missing discharge data.

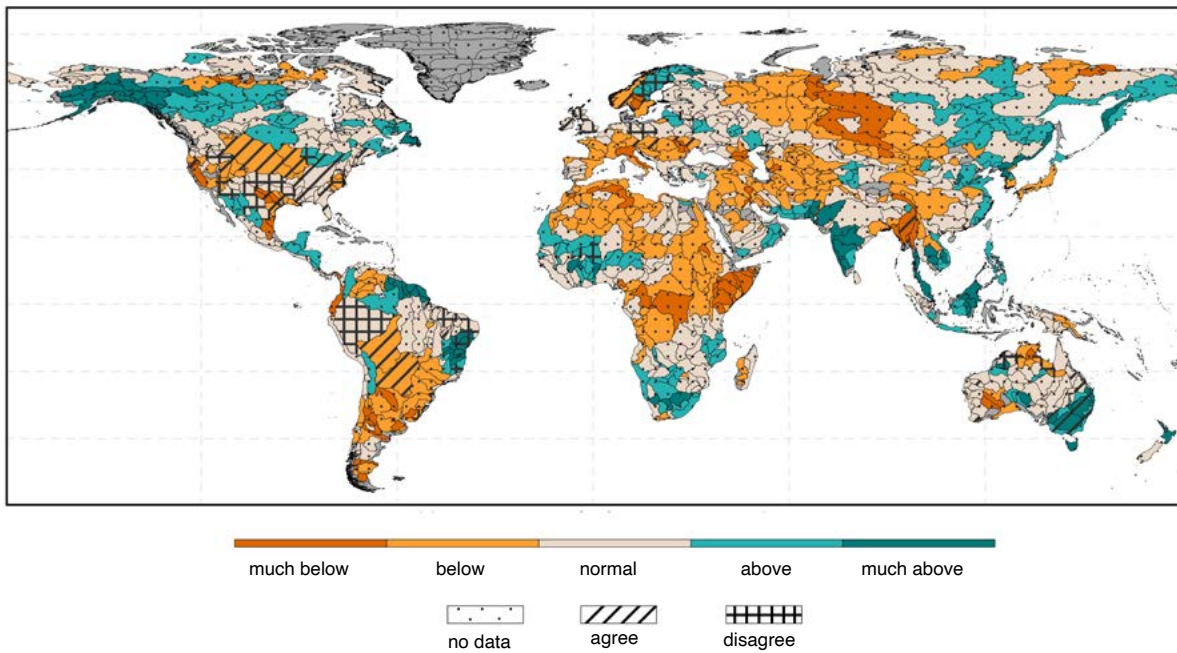


Figure A6. Validation of trend simulations for 2022 discharge. Areas where simulated and observed trends agree on the direction of change indicated by hatching.



The validation of modelled results showed agreement between observed and simulated anomalies for the year 2022 in Myanmar, Australia, the eastern and central United States, Central Europe, and upstream of La Plata basin. At the same time modelled trends disagree with observations in the Niger basin, northern Amazon and coastal area of Brazil, northern United States, Great Britain and Northern Europe. In general, GHMS simulations align with observations in 63% of the basins.

In some areas (for example, Great Britain and Northern Ireland) there was a mismatch between the resolution of the models (catchments above 10 000 km² were selected for the analysis) and the observed datasets. From Figure A5 it is evident that the entire territory of Great Britain is represented by just two basins in the models' setup; however data from seven observed stations with catchment areas of less than 10 000 km² were supplied by the United Kingdom hydrometeorological service, of which the one with the biggest catchment area was selected. This underlines the importance of improving the local information: from better spatial representation of relevant catchments to receiving and including in analysis observed river discharge data from more sites.

RESERVOIRS

The modelled results for the inflow into 926 reservoirs globally were obtained from four main sources: Global Water Watch,³⁴ Wflow_sbm,³⁵ CaMa-Flood with Dam^{36,37} and WWH.³⁸ The reservoirs were selected based on overlap between those three sources and identified by their GRanD id.³⁹ Daily inflow into selected GRanD reservoirs has been computed for the period 1991–2022.

Global Water Watch (<https://www.globalwaterwatch.earth/>): This source utilizes multi-year, multi-sensor satellite data (medium-resolution satellite images acquired in the last 35 years by NASA's Landsat and ESA's Copernicus Sentinel missions) alongside cloud analytics to globally monitor artificial water reservoirs. The data set is verified using 768 daily on-site water-level and storage measurements ($r^2 > 0.7$ for 67% of the reservoirs used in the validation).⁴⁰

Wflow_sbm:⁴¹ Daily inflow and daily reservoir volumes were calculated for the period 1991–2022 for the selected GRanD reservoirs.

CaMa-Flood with Dam: The CaMa-Flood model⁴² along with the Dam operational scheme by Hanazaki et al.⁴³ was used to conduct global simulations. The model can simulate river flows encompassing 2 169 global dams and reservoirs with a drainage area of at least 1 000 km². The information for each reservoir, such as dam name, coordinates, storage capacity and drainage area, in the model is based on information from GRanD.⁴⁴ The model configuration, done by Hanazaki et al.,⁴⁵ enables global simulations at a spatial resolution of 0.25° using MERIT Hydro⁴⁶ as a baseline topography. The same model configuration settings, utilizing ERA5-Land reanalysis data⁴⁷ from 1991 to 2022 for runoff forcing, have been used for the current global simulations. The temporal resolution of the model is one hour. However, keeping in view the reporting requirements, the outputs have been prepared at 24-hour intervals.

Calibration of the model with the Dam operational scheme is unavailable. However, Hanazaki et al.⁴⁸ conducted model validation based on simulations spanning 2001 to 2019. Validation for the model is accessible for the daily streamflow discharge of 687 gauges (located downstream of dams) from GRDC and other institutions worldwide. The accuracy of discharge hydrographs compared to observations was evaluated by calculating Nash–Sutcliffe efficiency (NSE)⁴⁹



and peak discharge error (PDE).⁵⁰ In addition to the 687 global gauges, validation is also available for inflow, outflow and storage at the Seminole and Trinity reservoirs using in situ observation data.

World-wide HYPE v1.3.9: Daily inflow into GRanD reservoirs and daily reservoir volume have been delivered for the period 1991–2022.

Figure A7 presents anomalies derived from the Global Water Watch data set; the map shows observed reservoir surface water area variations throughout each month of the year 2022. Calculation of climatological surface areas allows quantification of deviations from the normal pattern, measured in terms of standard deviations.

GROUNDWATER

Due to data constraints and for piloting purposes, a single trend has been calculated over a 10-year period from 1 January 2013 to 31 December 2022.

Ranking and trends were computed for groundwater levels, with observation wells grouped by aquifer. Groundwater levels at each well are averaged into mean monthly values, and time series with significant data gaps are excluded. These include series with fewer than four monthly values per year on average, and more than one year without data.

Monthly mean groundwater levels are normalized, averaged over the aquifer, and fitted with a linear trend. This trend's slope is classified as rising, stable or declining according to specific criteria:

- Rising: slope > 0.1 m/yr
- Stable: $-0.1 \text{ m/yr} < \text{slope} < 0.1 \text{ m/yr}$
- Declining: slope < -0.1 m/yr

The mean yearly value for 2022 is ranked against previous years' mean yearly values, with normalized groundwater levels averaged per year. Aquifer size is divided by the number of observation wells to estimate monitoring data representativity.

For this pilot, a 10-year timespan was analysed, which may not capture long-term water level dynamics in some aquifers. Future editions will use longer time series where available to address this issue.

SOIL MOISTURE

The soil moisture (topsoil, 5 cm) and evapotranspiration (see the following section) data sets are obtained from a global water cycle reanalysis product at 10 km spatial resolution. The same percentile ranking algorithm as was used for streamflow and reservoir inflow was used to generate the corresponding anomalies for 2022 based on the climatology of 2003–2020. The reanalysis product was created using the NASA Land Information System modelling framework^{51,52,53} by assimilating soil moisture data from the European Space Agency Climate Change Initiative (ESA CCI), leaf area index data from the Moderate Resolution Imaging Spectroradiometer (MODIS), and terrestrial water storage anomalies from Gravity Recovery and Climate Experiment and the follow-on satellites (GRACE/GRACE-FO).

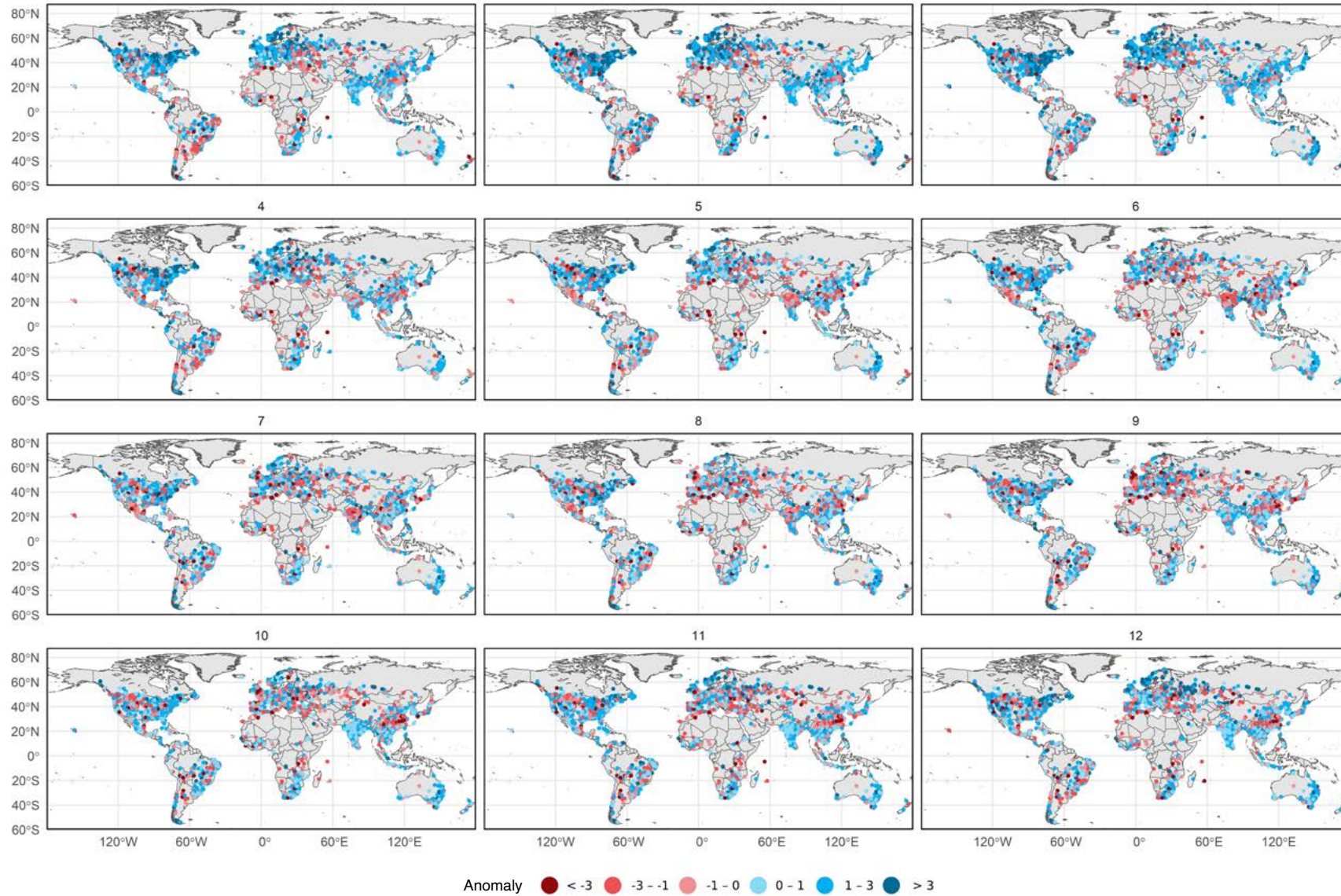


Figure A7. Monthly observed anomalies in reservoir surface areas for the year 2022, derived from the Global Water Watch dataset (<https://www.globalwaterwatch.earth/>). Anomalies are quantified in terms of the number of standard deviations from the norm.

Figure A8 presents the annual average anomaly in surface soil moisture in 2022 as ranked with respect to the historical period 2003–2020.

EVAPOTRANSPIRATION

Figure A9 presents the annual anomaly in evapotranspiration in 2022 as ranked with respect to the historical period 2003–2020.

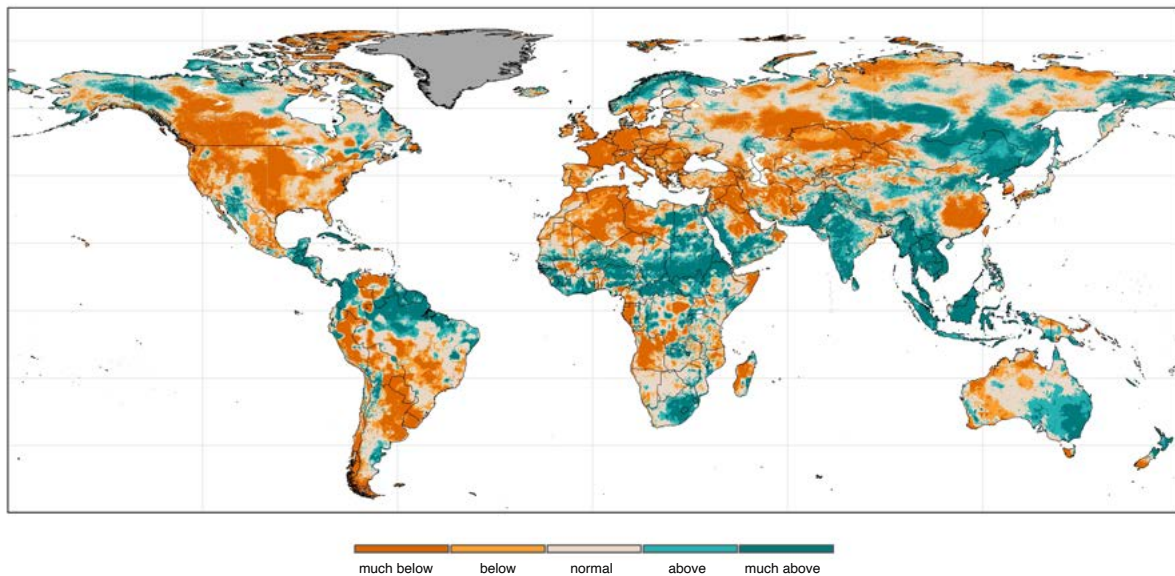


Figure A8. Annual anomaly in surface soil moisture in 2022 as ranked with respect to the historical period 2003–2020

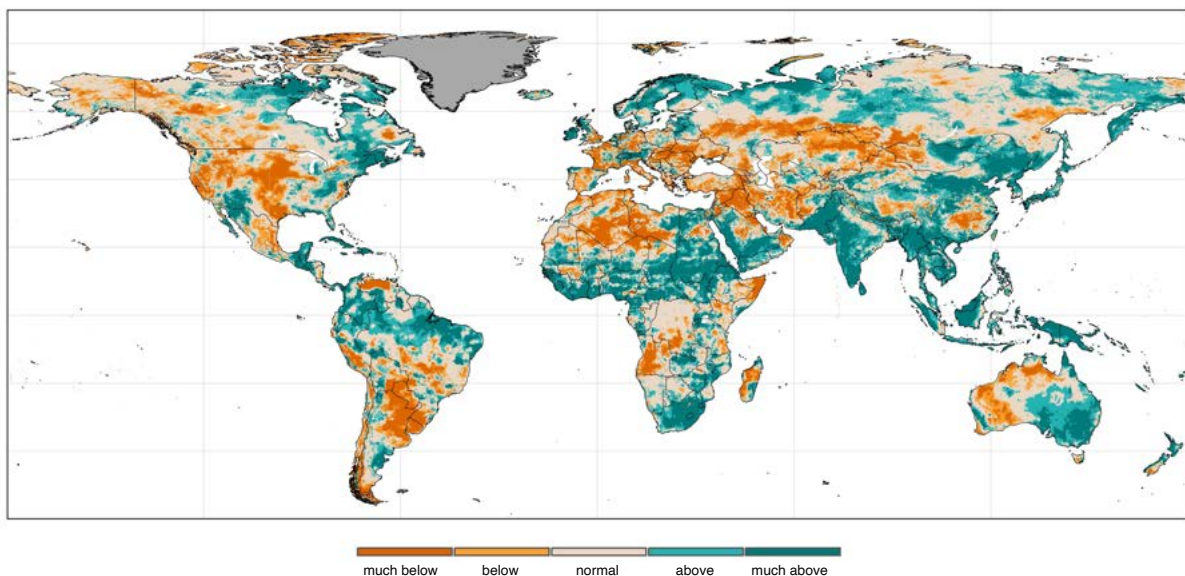


Figure A9. Annual anomaly in evapotranspiration in 2022 as ranked with respect to the historical period 2003–2020



TERRESTRIAL WATER STORAGE

Satellite gravimetry is the only remote-sensing-based method capable of observing the whole water column, including surface water, soil moisture, groundwater, and snow and ice. This report presents an analysis of the TWS anomaly between the years 2002 and 2021, observed with the Gravity Recovery and Climate Experiment (GRACE) mission (2002–2017) and its successor GRACE-Follow-On (Grace-FO) (since 2018).^{54,55,56} The GRACE data provide the TWS anomaly compared to the baseline of 2004–2009, and then the equation is used to adjust the TWS anomaly compared to the baseline of 2002–2020.

The TWS anomaly in equivalent water heights in centimetres was calculated according to the following formula:

$$TWS_{anomaly} = TWS_t - \bar{X}$$

where TWS_t (cm) is the TWS value of the month t of the current year, and \bar{X} is the long-term average TWS (cm), as calculated for 2002–2020. Equivalent water height is the theoretical mean height of the water column over the whole area being considered.

TWS for the year 2021 was ranked in a manner similar to that used for discharge. However, the time series of TWS data were too short (19 years) to perform ranking on the yearly values, therefore an index for each month was computed and then aggregated to the yearly mean values.

Endnotes

- ¹ Lehner, B.; Verdin, K.; Jarvis, A. New Global Hydrography Derived from Spaceborne Elevation Data. *Eos, Transactions American Geophysical Union* **2008**, *89*(10), 93–94. <https://doi.org/10.1029/2008EO100001>.
- ² Global Runoff Data Centre (GRDC). *WMO Basins and Sub-Basins*; 3rd rev. ext. ed., Federal Institute of Hydrology (BfG): Koblenz, Germany, 2020.
- ³ Data courtesy of the Global Runoff Data Centre, Koblenz, Germany.
- ⁴ van Verseveld, W. J.; Weerts, A. H.; Visser, M. et al. Wflow_sbm v0.6.1, a Spatially Distributed Hydrologic Model: From Global Data to Local Applications. *Geoscientific Model Development Discussions* **2022**, 1–52. <https://doi.org/10.5194/gmd-2022-182>.
- ⁵ Yamazaki, D.; Kanae, S.; Kim, H. et al. A Physically Based Description of Floodplain Inundation Dynamics in a Global River Routing Model. *Water Resources Research* **2011**, *47*(4). <https://doi.org/10.1029/2010WR009726>.
- ⁶ Arheimer, B.; Pimentel, R.; Isberg, K. et al. Global Catchment Modelling Using World-Wide HYPE (WWH), Open Data, and Stepwise Parameter Estimation. *Hydrology and Earth System Sciences* **2020**, *24*(2), 535–559. <https://doi.org/10.5194/hess-24-535-2020>.
- ⁷ Landerer, F. W.; Flechtner, F. M.; Save, H. et al. Extending the Global Mass Change Data Record: GRACE Follow-On Instrument and Science Data Performance. *Geophysical Research Letters* **2020**, *47*(12), e2020GL088306. <https://doi.org/10.1029/2020GL088306>.
- ⁸ Boergens, E.; Güntner, A.; Dobslaw, H. et al. Quantifying the Central European Droughts in 2018 and 2019 With GRACE Follow-On. *Geophysical Research Letters* **2020**, *47*(14), e2020GL087285. <https://doi.org/10.1029/2020GL087285>.
- ⁹ EM-DAT, CRED/UCLouvain, Brussels, Belgium. <http://www.emdat.be>.
- ¹⁰ Kumar, S. V.; Mocko, D. M.; Wang, S. et al. Assimilation of Remotely Sensed Leaf Area Index into the Noah-MP Land Surface Model: Impacts on Water and Carbon Fluxes and States over the Continental United States. *Journal of Hydrometeorology* **2019**, *20*(7), 1359–1377. <https://doi.org/10.1175/JHM-D-18-0237.1>.
- ¹¹ Arheimer, B.; Pimentel, R.; Isberg, K. et al. Global Catchment Modelling Using World-Wide HYPE (WWH), Open Data, and Stepwise Parameter Estimation. *Hydrology and Earth System Sciences* **2020**, *24*(2), 535–559. <https://doi.org/10.5194/hess-24-535-2020>.
- ¹² Müller Schmied, H.; Cáceres, D.; Eisner, S. et al. The Global Water Resources and Use Model WaterGAP v2.2d: Model Description and Evaluation. *Geoscientific Model Development* **2021**, *14*(2), 1037–1079. <https://doi.org/10.5194/gmd-14-1037-2021>.
- ¹³ Müller Schmied, H.; Cáceres, D.; Eisner, S. et al. The Global Water Resources and Use Model WaterGAP v2.2d: Model Description and Evaluation. *Geoscientific Model Development* **2021**, *14*(2), 1037–1079. <https://doi.org/10.5194/gmd-14-1037-2021>.
- ¹⁴ Yuan, X.; Ji, P.; Wang, L.; Liang, X.-Z.; Yang, K.; Ye, A.; Su, Z.; Wen, J. High-Resolution Land Surface Modeling of Hydrological Changes Over the Sanjiangyuan Region in the Eastern Tibetan Plateau: 1. Model Development and Evaluation. *Journal of Advances in Modeling Earth Systems* **2018**, *10*(11), 2806–2828. <https://doi.org/10.1029/2018MS001412>.
- ¹⁵ Samaniego, L.; Kumar, R.; Attinger, S. Multiscale Parameter Regionalization of a Grid-Based Hydrologic Model at the Mesoscale. *Water Resources Research* **2010**, *46*(5). <https://doi.org/10.1029/2008WR007327>.
- ¹⁶ Kumar, R.; Samaniego, L.; Attinger, S. Implications of Distributed Hydrologic Model Parameterization on Water Fluxes at Multiple Scales and Locations. *Water Resources Research* **2013**, *49*(1), 360–379. <https://doi.org/10.1029/2012WR012195>.
- ¹⁷ Samaniego, L.; Kaluza, M.; Kumar, R. et al. Mesoscale Hydrologic Model, 2019. <https://doi.org/10.5281/zenodo.3239055>.
- ¹⁸ Murray, A. M.; Jørgensen, G. H.; Godiksen, P. N. et al. DHI-GHM: Real-Time and Forecasted Hydrology for the Entire Planet. *Journal of Hydrology* **2023**, *620*, 129431. <https://doi.org/10.1016/j.jhydrol.2023.129431>.
- ¹⁹ Hanazaki, R.; Yamazaki, D.; Yoshimura, K. Development of a Reservoir Flood Control Scheme for Global Flood Models. *Journal of Advances in Modeling Earth Systems* **2022**, *14*(3), e2021MS002944. <https://doi.org/10.1029/2021MS002944>.
- ²⁰ Yamazaki, D.; Kanae, S.; Kim, H. et al. A Physically Based Description of Floodplain Inundation Dynamics in a Global River Routing Model. *Water Resources Research* **2011**, *47*(4). <https://doi.org/10.1029/2010WR009726>.



- ²¹ Yoshimura, K.; Sakimura, T.; Oki, T. et al. Toward Flood Risk Prediction: A Statistical Approach Using a 29-Year River Discharge Simulation over Japan. *Hydrological Research Letters* **2008**, *2*, 22–26. <https://doi.org/10.3178/hrl.2.22>.
- ²² Ma, W.; Ishitsuka, Y.; Takeshima, A. et al. Applicability of a Nationwide Flood Forecasting System for Typhoon Hagibis 2019. *Sci Rep* **2021**, *11* (1), 10213. <https://doi.org/10.1038/s41598-021-89522-8>.
- ²³ Alfieri, L.; Burek, P.; Dutra, E. et al. GloFAS – Global Ensemble Streamflow Forecasting and Flood Early Warning. *Hydrology and Earth System Sciences* **2013**, *17* (3), 1161–1175. <https://doi.org/10.5194/hess-17-1161-2013>.
- ²⁴ Grimaldi, S.; Salamon, P.; Disperati, J. et al. (2022): GloFAS v4.0 Hydrological Reanalysis; European Commission, Joint Research Centre (JRC) [Dataset]. <http://data.europa.eu/89h/f96b7a19-0133-4105-a879-0536991ca9c5>.
- ²⁵ Boussetta, S.; Balsamo, G.; Arduini, G. et al. ECLand: The ECMWF Land Surface Modelling System. *Atmosphere* **2021**, *12* (6), 723. <https://doi.org/10.3390/atmos12060723>
- ²⁶ Kumar, S. V.; Mocko, D. M.; Wang, S. et al. Assimilation of Remotely Sensed Leaf Area Index into the Noah-MP Land Surface Model: Impacts on Water and Carbon Fluxes and States over the Continental United States. *Journal of Hydrometeorology* **2019**, *20* (7), 1359–1377. <https://doi.org/10.1175/JHM-D-18-0237.1>.
- ²⁷ van Verseveld, W. J.; Weerts, A. H.; Visser, M. et al. Wflow_sbm v0.6.1, a Spatially Distributed Hydrologic Model: From Global Data to Local Applications. *Geoscientific Model Development Discussions* **2022**, 1–52. <https://doi.org/10.5194/gmd-2022-182>.
- ²⁸ Imhoff, R. O.; van Verseveld, W. J.; van Osnabrugge, B. et al. Scaling Point-Scale (Pedo)Transfer Functions to Seamless Large-Domain Parameter Estimates for High-Resolution Distributed Hydrologic Modeling: An Example for the Rhine River. *Water Resources Research* **2020**, *56* (4), e2019WR026807. <https://doi.org/10.1029/2019WR026807>.
- ²⁹ Eilander, D.; van Verseveld, W.; Yamazaki, D. et al. A Hydrography Upscaling Method for Scale-Invariant Parametrization of Distributed Hydrological Models. *Hydrology and Earth System Sciences* **2021**, *25* (9), 5287–5313. <https://doi.org/10.5194/hess-25-5287-2021>.
- ³⁰ Pomeroy, J. W.; Brown, T.; Fang, X. et al. The Cold Regions Hydrological Modelling Platform for Hydrological Diagnosis and Prediction Based on Process Understanding. *Journal of Hydrology* **2022**, *615*, 128711. <https://doi.org/10.1016/j.jhydrol.2022.128711>.
- ³¹ Hersbach, H.; Bell, B.; Berrisford, P. et al. The ERA5 Global Reanalysis. *Quarterly Journal of the Royal Meteorological Society* **2020**, *146* (730), 1999–2049. <https://doi.org/10.1002/qj.3803>.
- ³² Berg, P.; Almén, F.; Bozhinova, D. HydroGFD3.0 (Hydrological Global Forcing Data): A 25 km Global Precipitation and Temperature Data Set Updated in near-Real Time. *Earth System Science Data* **2021**, *13* (4), 1531–1545. <https://doi.org/10.5194/essd-13-1531-2021>.
- ³³ Kobayashi, S.; Ota, Y.; Harada, Y. et al. The JRA-55 Reanalysis: General specifications and basic characteristics. *Journal of the Meteorological Society of Japan* **2015**, *93*, 5–48. <https://doi.org/10.2151/jmsj.2015-001>.
- ³⁴ Donchyts, G.; Winsemius, H.; Baart, F. et al. High-Resolution Surface Water Dynamics in Earth's Small and Medium-Sized Reservoirs. *Sci Rep* **2022**, *12* (1), 13776. <https://doi.org/10.1038/s41598-022-17074-6>.
- ³⁵ van Verseveld, W. J.; Weerts, A. H.; Visser, M. et al. Wflow_sbm v0.6.1, a Spatially Distributed Hydrologic Model: From Global Data to Local Applications. *Geoscientific Model Development Discussions* **2022**, 1–52. <https://doi.org/10.5194/gmd-2022-182>.
- ³⁶ Hanazaki, R.; Yamazaki, D.; Yoshimura, K. Development of a Reservoir Flood Control Scheme for Global Flood Models. *Journal of Advances in Modeling Earth Systems* **2022**, *14* (3), e2021MS002944. <https://doi.org/10.1029/2021MS002944>.
- ³⁷ Yamazaki, D.; Kanae, S.; Kim, H. et al. A Physically Based Description of Floodplain Inundation Dynamics in a Global River Routing Model. *Water Resources Research* **2011**, *47* (4). <https://doi.org/10.1029/2010WR009726>.
- ³⁸ Arheimer, B.; Pimentel, R.; Isberg, K. et al. Global Catchment Modelling Using World-Wide HYPE (WWH), Open Data, and Stepwise Parameter Estimation. *Hydrology and Earth System Sciences* **2020**, *24* (2), 535–559. <https://doi.org/10.5194/hess-24-535-2020>.
- ³⁹ Lehner, B.; Reidy Liermann, C.; Revenga, C. et al. *Global Reservoir and Dam Database, Version 1 (GRanDv1): Dams, Revision 01*; NASA Socioeconomic Data and Applications Center (SEDAC): Palisades, USA, 2011. <https://doi.org/10.7927/H4N877QK>.



- ⁴⁰ Donchyts, G.; Winsemius, H.; Baart, F. et al. High-Resolution Surface Water Dynamics in Earth's Small and Medium-Sized Reservoirs. *Sci Rep* **2022**, *12* (1), 13776. <https://doi.org/10.1038/s41598-022-17074-6>.
- ⁴¹ van Verseveld, W. J.; Weerts, A. H.; Visser, M. et al. Wflow_sbm v0.6.1, a Spatially Distributed Hydrologic Model: From Global Data to Local Applications. *Geoscientific Model Development Discussions* **2022**, 1–52. <https://doi.org/10.5194/gmd-2022-182>.
- ⁴² Yamazaki, D.; Kanae, S.; Kim, H. et al. A Physically Based Description of Floodplain Inundation Dynamics in a Global River Routing Model. *Water Resources Research* **2011**, *47* (4). <https://doi.org/10.1029/2010WR009726>.
- ⁴³ Hanazaki, R.; Yamazaki, D.; Yoshimura, K. Development of a Reservoir Flood Control Scheme for Global Flood Models. *Journal of Advances in Modeling Earth Systems* **2022**, *14* (3), e2021MS002944. <https://doi.org/10.1029/2021MS002944>.
- ⁴⁴ Lehner, B.; Liermann, C. R.; Revenga, C. et al. High-Resolution Mapping of the World's Reservoirs and Dams for Sustainable River-Flow Management. *Frontiers in Ecology and the Environment* **2011**, *9* (9), 494–502. <https://doi.org/10.1890/100125>.
- ⁴⁵ Hanazaki, R.; Yamazaki, D.; Yoshimura, K. Development of a Reservoir Flood Control Scheme for Global Flood Models. *Journal of Advances in Modeling Earth Systems* **2022**, *14* (3), e2021MS002944. <https://doi.org/10.1029/2021MS002944>.
- ⁴⁶ Yamazaki, D.; Ikeshima, D.; Sosa, J. et al. MERIT Hydro: A High-Resolution Global Hydrography Map Based on Latest Topography Dataset. *Water Resources Research* **2019**, *55* (6), 5053–5073. <https://doi.org/10.1029/2019WR024873>.
- ⁴⁷ Muñoz Sabater, J. ERA5-Land Hourly Data from 1950 to Present; Copernicus Climate Change Service (C3S) Climate Data Store (CDS): 2019. <https://doi.org/10.24381/cds.e2161bac>.
- ⁴⁸ Hanazaki, R.; Yamazaki, D.; Yoshimura, K. Development of a Reservoir Flood Control Scheme for Global Flood Models. *Journal of Advances in Modeling Earth Systems* **2022**, *14* (3), e2021MS002944. <https://doi.org/10.1029/2021MS002944>.
- ⁴⁹ Nash, J. E.; Sutcliffe, J. V. River Flow Forecasting through Conceptual Models Part I — A Discussion of Principles. *Journal of Hydrology* **1970**, *10* (3), 282–290. [https://doi.org/10.1016/0022-1694\(70\)90255-6](https://doi.org/10.1016/0022-1694(70)90255-6).
- ⁵⁰ Hanazaki, R.; Yamazaki, D.; Yoshimura, K. Development of a Reservoir Flood Control Scheme for Global Flood Models. *Journal of Advances in Modeling Earth Systems* **2022**, *14* (3), e2021MS002944. <https://doi.org/10.1029/2021MS002944>.
- ⁵¹ Nie, W.; Kumar, S. V.; Getirana, A. et al. Nonstationarity in the Global Terrestrial Water Cycle and its Interlinkages in the Anthropocene. *Research Square* **2023** [preprint].
- ⁵² *A Global Reanalysis for Water, Energy, and Carbon Cycle Variables Overview*. <https://www.earthdata.nasa.gov/dashboard/data-catalog/global-reanalysis-da>
- ⁵³ Kumar, S. V.; Peters-Lidard, C. D.; Tian, Y. et al. Land Information System: An Interoperable Framework for High Resolution Land Surface Modeling. *Environmental Modelling & Software* **2006**, *21* (10), 1402–1415. <https://doi.org/10.1016/j.envsoft.2005.07.004>.
- ⁵⁴ Tapley, B. D.; Watkins, M. M.; Flechtner, F. et al. Contributions of GRACE to Understanding Climate Change. *Nature Climate Change* **2019**, *9* (5), 358–369. <https://doi.org/10.1038/s41558-019-0456-2>.
- ⁵⁵ Landerer, F. W.; Flechtner, F. M.; Save, H. et al. Extending the Global Mass Change Data Record: GRACE Follow-On Instrument and Science Data Performance. *Geophysical Research Letters* **2020**, *47* (12), e2020GL088306. <https://doi.org/10.1029/2020GL088306>.
- ⁵⁶ Boergens, E.; Güntner, A.; Döbbslaw, H. et al. Quantifying the Central European Droughts in 2018 and 2019 With GRACE Follow-On. *Geophysical Research Letters* **2020**, *47* (14), e2020GL087285. <https://doi.org/10.1029/2020GL087285>.



Annex 2. Quantitative status of groundwater

For more information, please contact:

World Meteorological Organization

7 bis, avenue de la Paix – P.O. Box 2300 – CH 1211 Geneva 2 – Switzerland

**Strategic Communications Office
Cabinet Office of the Secretary-General**

Tel: +41 (0) 22 730 83 14 – Fax: +41 (0) 22 730 80 27

Email: communications@wmo.int

public.wmo.int